J Reprod Fertil 1976; 48: 205–207.

4. **Vom Saal FS, Finch CE.** Reproductive senescence: phenomena and mechanisms in mammals and selected veterbrates. In: Knobil E, Neill JD, Ewing LL, Greenwald GS, Markert CL, Pfaff DW (eds.), The Physiology of Reproduction. New York: Raven Press; 1988: 2351–2414.
5. **Krarup T, Pedersen T, Faber M.** Regulation of oocyte growth in the mouse vary. *Nature* 1969; 224: 187–188.
6. **Meredith S, Dudenhoeffer G, Butcher RL, Lerner SP, Walls T.** Unlateral ovariectomy increases loss of primordial follicles and is associated with increased metaestrous concentration of follicle-stimulating hormone in old rats. *Biol Reprod* 1992; 47: 162–168.
7. **Merchant H.** Rat gonadal and ovarian organogenesis with and without germ cell. An ultrastructural study. *Develop Biol* 1975; 44: 1–21.
8. **Hirshfield AN.** Relationship between the supply of primordial follicles and the onsest of follicular growth in rats. *Biol Reprod* 1994; 50: 421–428.
9. **Shirota M, Soda S, Katoh C, Asai S, Sato M, Ohta R, Watanabe G, Taya K, Shirota K.** Effects of reduction of the number of primordial follicles on follicular development to achieve puberty in female rats. *Reproduction* 2003; 125: 85–94.
10. **Maekawa A, Onodera H, Tanigawa H, Furuta K, Kanno J, Matsuoka C, Ogiu T, Hahashi Y.** Spontaneous neoplastic and non-neoplastic lesions in aging Donryu rats. *Jpn J Cancer Res (Gann)* 1986; 77: 882–890.
11. **Nagaoka T, Onodera H, Matsushima Y, Todate A, Shibutani M, Ogasawara H, Maekawa A.** Spontaneous uterine adenocarcinomas in aged rats and their relation to endocrine imbalance. *J Cancer Res Clin Oncol* 1990; 116: 623–628.
12. **Nagaoka T, Takeuchi M, Onodera H, Matsushima Y, Ando-Lu J, Maekawa A.** A sequential observation of spontaneous endometrial adenocarcinoma development in Donryu rats. *Toxicol Pathol* 1994; 22: 261–269.
13. **Ando-Lu J, Takahashi M, Imai S, Ishihara R, Kitamura T, Iijima T, Takano S, Nishiyama K, Suzuki K, Maekawa A.** High-yield induction of endometrial adenocarcinomas in Donryu rats by a single intra-uterine administration of N-ethyl-N'-nitro-N-nitrosoguanidine. *Jpn J Cancer Res* 1994; 85: 789–793.
14. **Yoshida M, Kudoh K, Katsuda S, Takahashi M, Ando J, Maekawa A.** Inhibitory effects of uterine endometrial carcinogenesis in Donryu rats by tamoxifen. *Cancer Lett* 1998; 134: 43–51.
15. **Pecorelli S, Benedet JL, Creasman WT, Shepherd JH.** FIGO staging of gynecologic cancer. *Int J Gynecol Obstet* 1999; 64: 5–10.
16. **Taya K, Mizokawa T, Matsui T, Sasamoto S.** Induction of superovulation in prepubertal female rats by anterior pituitary transplants. *J Reprod Fertil* 1983; 69: 265–270.
17. **Watanabe G, Taya K, Sasamoto S.** Dynamics of ovarian inhibin secretion during the oestrous cycle of the rat. *J Endocrinol* 1990; 126: 151–157.
18. **Hamada T, Watanabe G, Kokuho T, Taya K, Sasamoto S, Hasegawa Y, Miyamoto K, Igarashi M.** Radioimmunoassay of inhibin in various mammals. *J Endocrinol* 1989; 122: 697–704.
19. **Taya K, Watanabe G, Sasamoto S.** Radioimmunoassay for progesterone, testosterone and estradiol-17β using 125I-iodohistamine radioligands. *Jpn J Anim Reprod* 1985; 31: 186–197.
20. **Ritz ND, Krim M.** Acute myeloblastic transformation after busulfan treatment of chronic myelocytic leukemia. *NY State J Med* 1959; 15: 4602–4608.
21. **Oliner H, Schwartz R, Rubio F, Dameshek W.** Interstitial pulmonary fibrosis following busulfan therapy. *Am J Med* 1961; 31: 134–139.
22. **Nishiyama K, Ando-Lu J, Nishimura S, Takahashi M, Yoshida M, Sasahara K, Miyajima K, Maekawa A.** Initiating and promoting effects of concurrent oral administration of ethylenethiourea and sodium nitrite on uterine endometrial adenocarcinoma development in Donryu rats. *In Vivo* 1998; 12: 363–368.
23. **Katsuda S, Yoshida M, Saarinen N, Smeds A, Nakae D, Santti R, Maekawa A.** Chemopreventive effects of hydroxymetairesinol on uterine carcinogenesis in Donryu rats. *Exp Biol Med* 2004: 229: 417–424.
24. **Newbold RR, Bullock BC, McLachlan JA.** Exposure to diethylstilboestrol during pregnancy permanently alters the ovary and oviduct. *Biol Reprod* 1983; 28: 735–744.
25. **Katsuda S, Yoshida M, Watanabe G, Taha K, Maekawa A.** Irreversible effects of neonatal exposure to p-tert-octylphenol on the reproductive tract in female rats. *Toxicol Appl Pharmacol* 2000; 165: 217–226.
26. **Kraus FT.** Ovarian senescence, failure, atrophy. In: WAD Anderson, JM Kissane (eds.), Pathology, 7 edition. Missouri, USA: Mosby; 1977: 1730–1731.
27. **McLachlan RI, Cohen NL, Dahl KD, Bremner WJ, Soules MR.** Serum inhibin levels during the preovulatory interval in normal women: relationship with sex steroid and gonadotrophin levels. *Clin Endocrinol* 1990; 32: 39–48.
28. **Fraser HM, Wakeling AE, Dukes M.** Control of FSH secretion during the primate menstrual cycle: studies using a pure anti-estrogen and inhibin immunoneutralization. *Biol Reprod* 1993; 48: (Suppl. 1) Abst. 13.
29. **Noguchi J, Watanabe G, Taya K, Sasamoto S.** Suppression of basal secretion of FSH inhibits follicular development and maturation during the

oestrous cycle of the rat. *J Endocrinol* 1993; 139: 287–293.

30. **Watanabe G.** Control mechanisms of FSH secretion by inhibin in the rat. *Bull Fac Agri Tech* 1993; 31: 1–58 (In Japanese).
31. **Herath CB, Yamashita S, Watanabe G, Jin W, Tangtrongsup S, Kojima A, Groome NP, Suzuki AK, Taya K.** Regulation of follicle-stimulating hormone secretion by estradiol and dimeric inhibins in the infantile female rats. *Biol Reprod* 2001; 65: 1623–1633.
32. **Aksoy M, Erdem S, Bakioglu I, Dincol G.** Endometrial cancer due to busulfan therapy. Report of two cases. *J Cancer Res Clin Oncol* 1984;108: 362–363.
33. **Greco TL, Furlow JD, Dueello TM, Gorski J.** Immunohistochemical of estrogen receptors in fetal and neonatal female mouse reproductive tracts. *Endocrinol* 1991; 129: 1326–1332.
34. **Lubahn DB, Moyer JS, Golding TS, Couse JF, Korach KS, Smithies O.** Alteration of reproductive function but not prenatal sexual development after insertinal disruption of the mouse estrogen receptor gene. *Proc Natl Acad Aci USA* 1993; 90: 11162–11166.
35. **Yoshida M, Takenaka A, Katsuda S, Kurokawa Y, Maekawa A.** Neonatal exposure to p-tert-octylphenol causes abnormal expression of estrogen receptor α and subsequent alteration of cell proliferating activity in the developing Donryu rat uterus. *Toxicol Pathol* 2002; 30: 357–364.

J Toxicol Pathol 2005; 18: 47–52

Original

α-Smooth Muscle Actin-positive Stromal Cells Reactive to Estrogens Surround Endometrial Glands in Rats but not Mice

Takasumi Shimomoto[1], Midori Yoshida[1], Shin-ichi Katsuda[3], Masakazu Takahashi[1], Fumiyuki Uematsu[1], Hiroki Kuniyasu[4], Akihiko Maekawa[2], and Dai Nakae[1]

[1]Department of Pathology, Sasaki Institute, Sasaki Foundation, 2–2 Kanda-Surugadai, Chiyoda, Tokyo 101–0062, Japan
[2]Director, Sasaki Institute, Sasaki Foundation, 2–2 Kanda-Surugadai, Chiyoda, Tokyo 101–0062, Japan
[3]Department of Biological Safety Research, Tama laboratory, Japan Food Research Laboratories, 6–11–10 Nagayama, Tama, Tokyo 206–0025, Japan
[4]Department of Molecular Pathology, Nara Medical University, 840 Shijo-cho, Kashihara, Nara 634–8521, Japan

Abstract: In human endometrium, α-smooth muscle actin (α-SMA)-positive stromal cells (SMA-SCs) surround endometrial glands, and the α-SMA expression is regulated by estrogen. The biological significance of these cells remains to be elucidated, and no information is available with regard to their animal counterparts. The present study, therefore, investigated SMA-SCs in the uteri of female Donryu rats and CD-1 mice. SMA-SCs with morphological similarities to those in the human were detected around the endometrial glands in normal cycling rats, but not in mice. Furthermore, the rat SMA-SCs disappeared after ovariectomy but returned with estrogen replacement in a duration-dependent manner, suggesting the regulatory role of estrogens similar to the human situation. Thus, SMA-SCs are present in rats, but not in mice, with characteristics close to their human counterparts. Their biological significance now needs to be elucidated by comparative studies. (J Toxicol Pathol 2005; **18**: 47–52)

Key words: endometrial stromal cells, α-smooth muscle actin, 17β-estradiol, octylphenol, Donryu rat

Introduction

Actin, a cytoskeletal protein involved in cell contraction, cell movement and cell-to-substrate adhesion[1–6], has been divided into six isoforms: two non-muscle actins (β and γ) known to be cytoplasmic, two smooth muscle actins (α and γ), and two sarcomeric actins (α-cardiac and α-skeletal)[7–9]. The α-smooth muscle actin (α-SMA) is found in smooth muscle cells, pericytes and myoepithelial cells[10–12], and in humans normal endometrial stromal cells around endometrial glands have also been shown to immunostain for α-SMA[13,14]. This α-SMA expression in stromal cells changes during the estrous cycle, greater numbers of positive cells being present in the proliferative than in the secretory phase[13]. Furthermore, in the proliferative phase α-SMA-positive stromal cells (SMA-SCs) can be detected occasionally in the more superficial mucosa and around non-dilated glands as well as in the lower, basal layer of the endometrial mucosa and around dilated or cystic glands, whereas SMA-SCs in the secretory phase are mostly evident in the basal, inactive layer and around single non-secretory glands[14]. This suggests that estrogen influences α-SMA expression in the endometrial stromal cells, although their significance remains to be elucidated. Furthermore, no information is available in the literature about their existence in experimental animals, such as rodents. The present study was thus conducted to determine whether SMA-SCs are a feature of the uteri of rats and mice. Finding them present in rats, we then assessed the reactivity of SMA-SCs to 17β-estradiol and *p-tert*-octylphenol, an endocrine disrupting chemical with estrogenic activity, using ovariectomized rats.

Received: 10 November 2004, Accepted: 21 February 2005
Mailing address: Takasumi Shimomoto, Department of Pathology, Sasaki Institute, Sasaki Foundation, 2–2 Kanda-Surugadai, Chiyoda, Tokyo 101–0062, Japan
TEL: 81-3-3294-3286 FAX: 81-3-3294-3290
E-mail: pathol@sasaki.or.jp

Materials and Methods

Ethical considerations for animal experiments

The animal experiments conducted in this study were approved by the Animal Experimentation Committee of the Sasaki Institute prior to their execution and were conducted under monitoring by the committee in accordance with the National Institutes of Health Guidelines for the Care and Use of Laboratory Animals, Japanese Government Animal Protection and Management Law Number 105 and Japanese

Government Notification on Feeding and Safekeeping of Animals Number 6.

Animals

A total of 30 virgin female Donryu rats (Crj:Donryu, 6 or 10 weeks of age) and 12 virgin CD-1 mice (Crj:CD-1, 7 weeks of age) were purchased from Charles River Japan Inc. (Kanagawa, Japan). They were housed in plastic cages, kept in an air-conditioned animal room (under constant conditions of 24 ± 2°C, 55 ± 10% humidity, and a 12-hour light/dark cycle), and maintained on a basal diet, CRF-1 (Oriental Yeast Inc., Tokyo, Japan) with tap water *ad libitum*.

Experimental design

Experiment I: Twelve animals each of the two species showing normal estrous cyclicity were selected, and vaginal smears were checked every morning. At ages of 12 or 15 weeks (rats) and 9 weeks (mice), 3 animals each were euthanized in the 4 stages of the estrous cycle (proestrus, estrus, metestrus and diestrus), and the uteri were excised for histological and immunohistochemical examination. The uterine horns were fixed in 10% neutrally buffered formalin solution and embedded in paraffin. Appropriate numbers of serial sections at a thickness of 4 μm were then prepared from each specimen, one being routinely stained with hematoxylin and eosin for histological examination. The other sections were processed for immunohistochemical analyses using mouse monoclonal antibodies against α-SMA (clone 1A4, Dakocytomation Japan, Kyoto, Japan, 100-fold diluted) and cytokeratin 14 (CK14; clone LL002, Novocastra Laboratories Ltd., Newcastle upon Tyne, UK, 20-fold diluted), the latter for the rat uteri only, at 4°C overnight, then processed for the labeled polymer method using an Envision Plus kit (Dakocytomation) according to the manufacturer's instructions, and counterstained with hematoxylin. Negative controls were included with primary antibodies omitted.

Experiment II: At 8 weeks of age, 18 rats underwent ovariectomy via the dorsal route under light ether anesthesia. Three weeks after the operation, they were equally divided into 3 groups, given subcutaneous injections of vehicle (dimethylsulfoxide), 5 μg/kg/day of 17β-estradiol (E_2; Wako Pure Chemical Industries Ltd., Osaka, Japan) or 100 mg/kg/day of *p-tert*-octylphenol (OP; Wako), respectively, for 2 or 14 successive days (3 animals each). The animals were euthanized 24 hours after the last administration, and the uteri were excised. The uterine horns were processed in the same manner as for experiment I except that CK14 immunostaining was not performed.

Results

Experiment I

In rats, the endometrial stroma was cellular, especially in the subluminal layer surrounding the glandular epithelium. The stromal cells surrounding the glands were spindly in shape with oval or spindle nuclei, resembling fibroblasts rather than basket-shaped myoepithelial cells. They were arranged in one or several layers around the glands (Fig. 1A) in all stages of the estrous cycle. In mice, the endometrial stroma was also cellular, but stromal cells surrounding the endometrial glands were not very conspicuous (Fig. 2A).

Immunohistochemically, the stromal cells surrounding the endometrial glands in one or several layers were positive for α-SMA in rats (Figs. 1B and 1C). Positive cells were observed through all stages of the estrous cycle, but the cell layers were thickest in proestrus (Figs. 1B and 1C). The stromal cells were negative for CK14 (Fig. 1D). In mice, SMA-SCs were not detected at any stage of the estrous cycle (Fig. 2B). In the uteri of both rats and mice, smooth muscle fibers in the blood vessels and the myometrium were positive for α-SMA (Figs. 1B, 1C and 2B).

Experiment II

In the ovariectomized rats, the uteri were severely atrophic, and the luminal epithelial cells in the endometrium were cuboidal rather than columnar in shape. The endometrial stromal cells and smooth muscle in the myometrium were reduced in size (Fig. 3A). In rats treated with E_2 for 2 days, the size of the uteri recovered remarkably, and the luminal epithelial cells in the endometrium were again columnar in shape. The endometrial stromal cells also recovered, and the myometrium was multi-layered (Figs. 3A and 3B). In rats treated with E_2 for 14 days, the uteri were as large as those of 2-day-treated animals while the endometrial stromal cells were larger (Figs. 3B and 3C) and the myometrium was thicker (Figs. 3B and 3C). In rats receiving OP, the uteri generally demonstrated similar histological findings to those in the rats treated with E_2 for the same term (Figs. 3C and 3D).

Table 1 summarizes the data of the α-SMA immunohistochemistry of stromal cells surrounding the endometrial glands in experiment II. In ovariectomized rats treated with vehicle stromal cells were negative for α-SMA (Fig. 4A), but 2 out of 3 rats treated with E_2 for 2 days exhibited weakly-positive spindle cells around the glands (Fig. 4B). Furthermore, α-SMA-positive cells were observed in all rats injected with E_2 for 14 days (Fig. 4C). Similarly, one out of 3 rats treated with OP for 2 days and all rats receiving OP for 14 days had SMA-SCs (Fig. 4D). Smooth muscle fibers in the blood vessels and the myometrium were positive for α-SMA in rats of all groups (Figs. 4A-D).

Discussion

The present study unequivocally demonstrated the presence of SMA-SCs surrounding endometrial glands in untreated rats but not mice. The SMA-SCs clearly differed from myoepithelial cells, characterized as basket-shaped with a positive CK14 phenotype[15,16], and were similar to SMA-SCs in the human endometrium, negative for

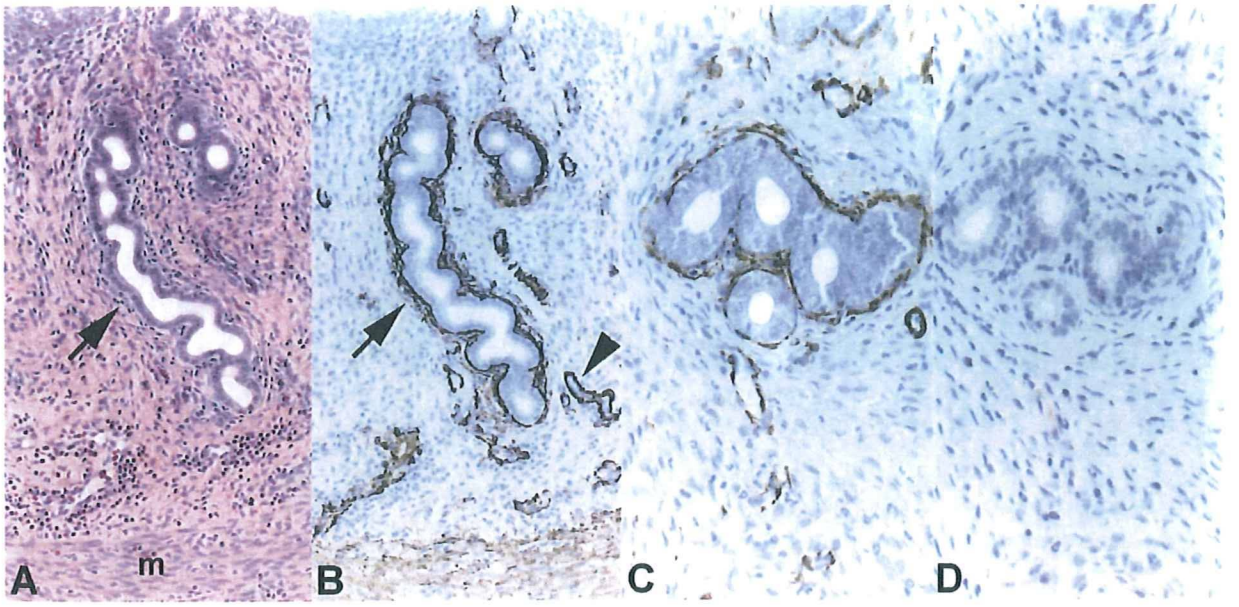

Fig. 1. Uteri of untreated rats (experiment I). (A) Representative histology in proestrus. Several layers of stromal cells surround endometrial glands (arrow). m: myometrium, × 90. (B) Representative α-SMA immunohistochemistry in proestrus. One or several layers of stromal cells surrounding endometrial glands are positive (arrow). Smooth muscle fibers in the blood vessels (arrowhead), as well as in the myometrium, are also positive, × 90. (C) Representative α-SMA immunohistochemistry in metestrus. One or two layers of stromal cells surrounding endometrial glands are positive, × 180. (D) Representative CK14 immunohistochemistry in metestrus. The endometrial stromal cells are negative, × 180.

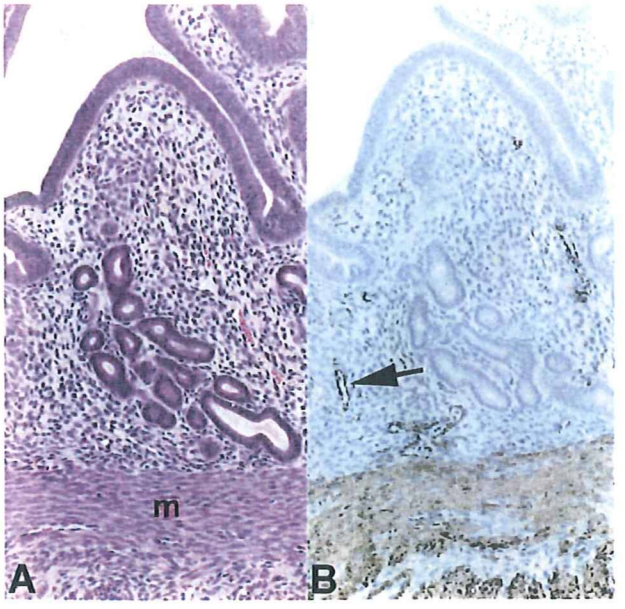

Fig. 2. Uteri of untreated mice (experiment I). (A) Representative histology in proestrus. Endometrial stromal cells are diffusely present throughout the stroma. m: myometrium, × 90. (B) Representative α-SMA immunohistochemistry in proestrus. The endometrial stromal cells are negative. Smooth muscle fibers in the blood vessels (arrow), as well as in the myometrium, are positive, × 90.

Table 1. Grades of α-SMA Immunohistochemistry for the Stromal Cells Surrounding Endometrial Glands in Ovariectomized Rats (Experiment II)

Group	Treatment		Grade		
	Compound	Period	–	±	+
1	Vehicle	2 days	3	0	0
		14 days	3	0	0
2	E_2	2 days	1	2	0
		14 days	0	0	3
3	OP	2 days	2	1	0
		14 days	0	0	3

Symbols used are: –, negative; ±, weakly positive; +, positive.

cytokeratins and distinguishable from myoepithelial cells[14]. Human SMA-SCs have been suggested to be a subset of myofibroblasts[13,14]. Myofibroblasts are characterized as having features of both smooth muscle cells and fibroblasts[17–19], and can be classified into 4 subtypes based on their differential immunoreactivity with antibodies against vimentin, desmin and α-SMA[20]. Results of the present study indicate that the SMA-SCs present in rats similarly have a myofibroblast origin, judging from the morphological findings.

In the rats, layers of SMA-SCs were apparent in proestrus, when serum E_2 levels are the highest of the estrous cycle. The fact that the endometrial stromal cells surrounding endometrial glands were small in size and negative for α-SMA in ovariectomized rats, with recovery

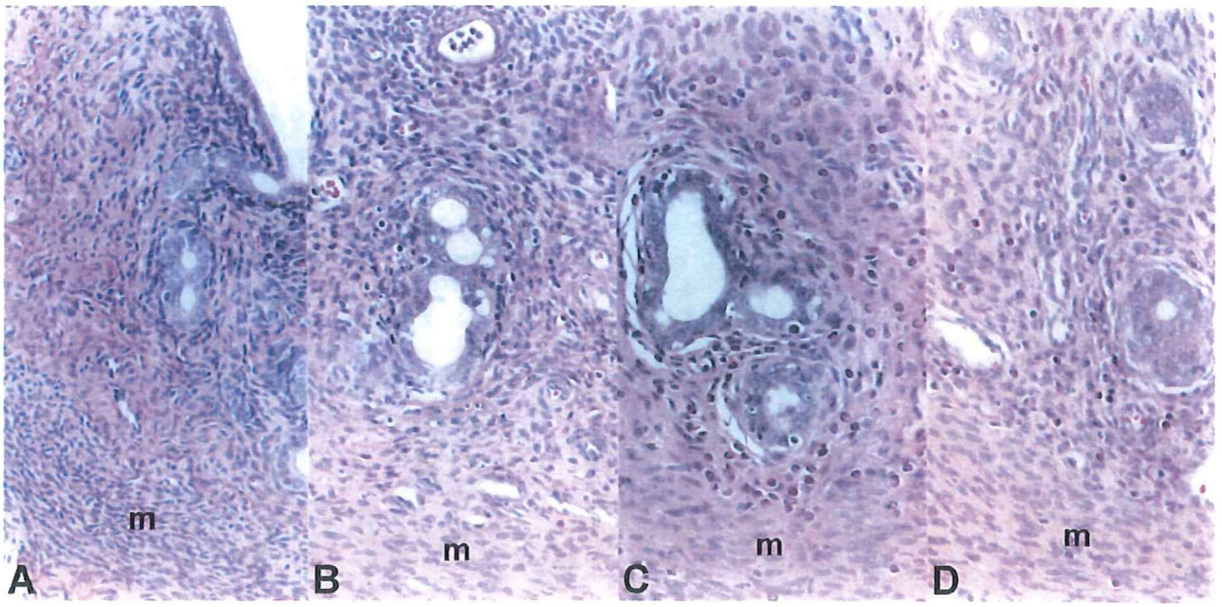

Fig. 3. Representative histology of uteri of ovariectomized rats (experiment II), × 180. (A) Treated with vehicle for 14 days. The endometrial stromal cells and smooth muscle in the myometrium (m) are small in size. (B) After treatment with E_2 for 2 days; the endometrial stromal cells are larger in size than those of the vehicle controls. Smooth muscle in the myometrium (m) is also thicker. (C) After treatment with E_2 for 14 days; the endometrial stromal cells are larger than those of the 2-day-treated rats and the myometrium (m) is thicker. (D) After treated with OP for 14 days; the endometrial stromal cells are large and the myometrium (m) is thick, like those of the rats receiving E_2 for 14 days.

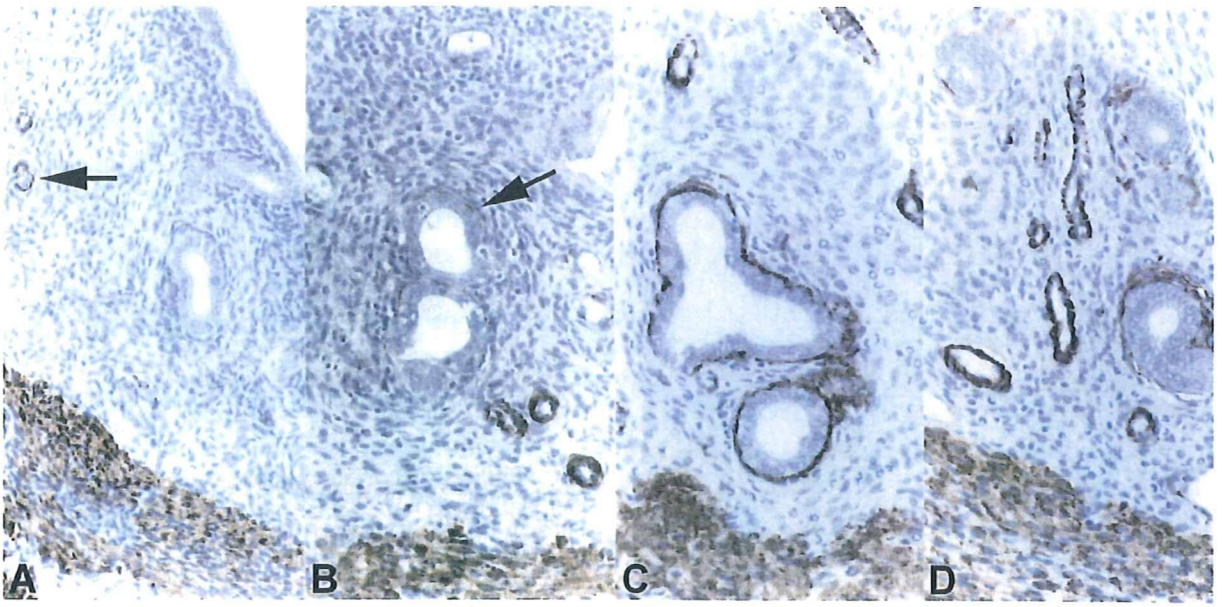

Fig. 4. Representative α-SMA immunohistochemistry of uteri of ovariectomized rats (experiment II), × 180. (A) Treated with vehicle for 14 days. Stromal cells surrounding endometrial glands are negative. Smooth muscle fibers in the blood vessels (arrow), as well as in the myometrium, are positive. (B) Treated with E_2 for 2 days. Some stromal cells surrounding endometrial glands are weakly positive (arrow). (C) Treated with E_2 for 14 days. One layer of the stromal cells surrounding endometrial glands is positive. (D) Treated with OP for 14 days. The stromal cells surrounding endometrial glands are positive.

on treatment with estrogen or OP, in a duration-dependent manner, clearly points to hormone dependence. OP is an endocrine disrupting chemical with estrogenic activity, from *in vitro* and *in vivo* evidence[21–28], and the dose of OP used in this study has been shown to be sufficient to exert estrogenic effects on the female reproductive tract in ovariectomized rats[27]. The results thus suggest that, similar to the human situation[13,14], estrogen modulates α-SMA expression in the

stromal cells surrounding endometrial glands in rats. Although the underlying mechanisms remain largely obscure, estrogen receptors can be immunohistochemically detected in endometrial stroma as well as in epithelium and in myometrium[29], and Hsu and Frankel[30] have demonstrated that mRNA expression of the *smooth muscle actin* gene is up-regulated by estrogens in immature rat uteri.

Myofibroblasts have been proposed as playing crucial roles in the contraction and relaxation of human granulation tissue on the basis of *in vitro* pharmacological reactivity similar to the smooth muscle[2]. α-SMA-positive myofibroblasts are also observed in rat granulation tissue[18] and may act similarly to their human counterparts. α-SMA is also expressed in passaged cultures of chick embryo fibroblasts[10], and stress fibers containing actin have been postulated as playing structural roles in the connection of the cytoplasmic matrix to the substrate rather than being contractile[4]. Thus, SMA-SCs surrounding endometrial glands might either participate in the contraction of glands or in the cell's adhesion to the surrounding substrate. Mechanistic studies are now needed to clarify, for example, the lack of SMA-SCs in mice.

In conclusion, SMA-SCs are present in rats, but not mice, and surround the endometrial glands, exhibiting morphological and endocrinological similarities to their human counterparts. Elucidation of their functional significance now needs to be performed by comparative studies in different species.

Acknowledgments: The authors would like to express their gratitude to Ms. Hiromi Asako, Hiromi Ichihara and Chinami Kajiwara (alphabetical order of surnames) for their expert technical assistance. This work was supported in part by Grants-in-Aid for Cancer Research Designate 14-5 (to D.N.) and Health and Labor Sciences Research Grant, Research on Food and Chemical Safety 44 (to M.Y.), both from the Ministry of Health, Labor and Welfare of Japan.

References

1. Buckley IK and Porter KR. Cytoplasmic fibrils in living cultured cells. A light and electron microscope study. Protoplasma. **64**: 349–380. 1967.
2. Ryan GB, Cliff WJ, Gabbiani G, Irlé C, Montandon D, Statkou PR, and Majno G. Myofibroblasts in human granulation tissue. Human Pathol. **5**: 55–67. 1974.
3. Geiger B. A 130K protein from chicken gizzard: its localization at the termini of microfilament bundles in cultured chicken cells. Cell. **18**: 193–205. 1979.
4. Herman IM, Crisona NJ, and Pollard TD. Relation between cell activity and the distribution of cytoplasmic actin and myosin. J Cell Biol. **90**: 84–91. 1981.
5. Willingham MC, Yamada SS, Davies PJA, Rutherford AV, Gallo MG, and Pastan I. Intracellular localization of actin in cultured fibroblasts by electron microscopic immunocytochemistry. J Histo Cytochem. **29(1)**: 17–37. 1981.
6. Hynes RO, Destree AT, and Wagner DD. Relationships between microfilaments, cell-substratum adhesion, and fibronectin. Cold Spring Harbor Symp Quant Biol. **46**: 659–670. 1982.
7. Vandekerckhove J and Weber K. At least six different actins are expressed in a higher mammal: an analysis based on the amino acid sequence of the amino-terminal tryptic peptide. J Mol Biol. **126**: 783–802. 1978.
8. Vandekerckhove J and Weber K. The complete amino acid sequence of actins from bovine aorta, bovine heart, bovine fast skeletal muscle, and rabbit slow skeletal muscle. A protein-chemical analysis of muscle actin differentiation. Differentiation. **14**: 123–133. 1979.
9. Vandekerckhove J and Weber K. Actin typing on total cellular extracts. A highly sensitive protein-chemical procedure able to distinguish different actins. Eur J Biochem. **113**: 595–603. 1981.
10. Skalli O, Ropraz P, Trzeciak A, Benzonana G, Gillessen D, and Gabbiani G. A monoclonal antibody against α-smooth muscle actin: a new probe for smooth muscle differentiation. J Cell Biol. **103(6)**: 2787–2796. 1986.
11. Skalli O, Pelte M, Peclet M, Gabbiani G, Gugliotta P, Bussolati G, Ravazzola M, and Orci L. α-smooth muscle actin, a differentiation marker of smooth muscle cells, is present in microfilamentous bundles of pericytes. J Histo Cytochem. **37(3)**: 315–321. 1989.
12. Gugliotta P, Sapino A, Macrí L, Skalli O, Gabbiani G, and Bussolati G. Specific demonstration of myoepithelial cells by anti-alpha smooth muscle actin antibody. J Histo Cytochem. **36(6)**: 659–663. 1988.
13. Franquemont DW, Frierson HF, and Mills SE. An immunohistochemical study of normal endometrial stroma and endometrial stromal neoplasms. Evidence for smooth muscle differentiation. Am J Surg Pathl. **15(9)**: 861–870. 1991.
14. Czernobilsky B, Remadi S, and Gabbiani G. Alpha-smooth muscle actin and other stromal markers in endometrial mucosa. Virchows Archiv A Pathol Anat. **422**: 313–317. 1993.
15. Dairkee SH, Blayney C, Smith HS, and Hackett AJ. Monoclonal antibody that defines human myoepithelium. Proc Natl Acad Sci. **82**: 7409–7413. 1985.
16. Shimomoto T, Yoshida M, Takahashi M, and Maekawa A. Sebaceous gland metaplasia in a mammary fibroadenoma developing in a female Donryu rat. J Toxicol Pathol. **15**: 73–77. 2002.
17. Gown AM. Editorial. The mysteries of the myofibroblast (partially) unmasked. Lab Invest. **63(1)**: 1–3. 1990.
18. Darby I, Skalli O, and Gabbiani G. α-smooth muscle actin is transiently expressed by myofibroblasts during experimental wound healing. Lab Invest. **63(1)**: 21–29. 1990.
19. Schürch W, Seemayer TA, and Gabbiani G. Chapter 5. Myofibroblasts. In: Histology for Pathologists. SS Sternberg (ed). Raven Press, New York. 109–144. 1992.
20. Skalli O, Schürch W, Seemayer T, Lagacé R, Montandon D, Pittet B, and Gabbiani G. Myofibroblasts from diverse pathologic settings are heterogeneous in their content of actin isoforms and intermediate filament proteins. Lab Invest. **60(2)**: 275–285. 1989.
21. Soto AM, Sonnenschein C, Chung KL, Fernandez MF, Olea N, and Serrano FO. The E-SCREEN assay as a tool to identify estrogens: an update on estrogenic environmental pollutants. Environ Health Perspect. **103**(Suppl 7): 113–122.

1995.
22. Kwack SJ, Kwon O, Kim HS, Kim SS, Kim SH, Sohn KH, Lee RD, Park CH, Jeung EB, An BS, and Park KL. Comparative evaluation of alkylphenolic compounds on estrogenic activity in vitro and in vivo. J Toxicol Environ Health A. **65**: 419–431. 2002.
23. White R, Jobling S, Hoare SA, Sumpter JP, and Parker MG. Environmentally persistent alkylphenolic compounds are estrogenic. Endocrinology. **135(1)**: 175–182. 1994.
24. Blake CA and Boockfor FR. Chronic administration of the environmental pollutant 4-tert-octylphenol to adult male rats interferes with the secretion of luteinizing hormone, follicle-stimulating hormone, prolactin, and testosterone. Biol Reprod. **57**: 255–266. 1997.
25. Boockfor FR and Blake CA. Chronic administration of 4-tert-octylphenol to adult male rats causes shrinkage of the testes and male accessory sex organs, disrupts spermatogenesis, and increases the incidence of sperm deformities. Biol Reprod. **57**: 267–277. 1997.
26. Blake CA and Ashiru OA. Disruption of rat estrous cyclicity by the environmental estrogen 4-tert-octylphenol. Proc Soc Exp Bio Med. **216**: 446–451. 1997.
27. Katsuda S, Yoshida M, Isagawa S, Asagawa Y, Kuroda H, Watanabe T, Ando J, Takahashi M, and Maekawa A. Dose- and treatment duration-related effects of p-tert-octylphenol on female rats. Reprod Toxicol. **14**: 119–126. 2000.
28. Yoshida M, Katsuda S, Ando J, Kuroda H, Takahashi M, and Maekawa A. Subcutaneous treatment of p-tert-octylphenol exerts estrogenic activity on the female reproductive tract in normal cycling rats of two different strains. Toxicol Lett. **116**: 89–101. 2000.
29. Wang H, Eriksson H, and Sahlin L. Estrogen receptors alpha and beta in the female reproductive tract of the rat during the estrous cycle. Biol Reprod. **63(5)**: 1331–1340. 2000.
30. Hsu CJ and Frankel FR. Effect of estrogen on the expression of mRNAs of different actin isoforms in immature rat uterus. J Biol Chem. **262(20)**: 9594–9600. 1987.

Distinct patterns of gene expression in hepatocellular carcinomas and adjacent non-cancerous, cirrhotic liver tissues in rats fed a choline-deficient, L-amino acid-defined diet

Fumiyuki Uematsu,[1,8] Masakazu Takahashi,[1] Midori Yoshida,[1] Maki Igarashi,[1,2] Naoto Watanabe,[1,2] Noriko Suzuki,[1,3] Masayoshi Abe,[1,4] Ivan Rusyn,[5] Robert A. Floyd[6,7] and Dai Nakae[1]

[1]Department of Pathology, Sasaki Institute, Sasaki Foundation, 2-2 Kanda-Surugadai, Chiyoda-ku, Tokyo 101-0062; [2]Laboratory of Protection of Body Function, Department of Food and Nutritional Science, Graduate School of Agriculture, Tokyo University of Agriculture, 1-1-1 Sakuragaoka, Setagaya-ku, Tokyo 156-8502; [3]Department of Nutritional Sciences, Faculty of Applied Bio-Science, Tokyo University of Agriculture, 1-1-1 Sakuragaoka, Setagaya-ku, Tokyo 156-8502; [4]Toxicology Group, Toxicology and Environmental Science Department, Biological Research Laboratories, Nissan Chemical Industries, 1470 Shiraoka, Saitama 349-0294, Japan; [5]Department of Environmental Sciences and Engineering, School of Public Health, University of North Carolina, Chapel Hill, NC 27599-7431; [6]Free Radical Biology and Aging Research Program, Oklahoma Medical Research Foundation, Oklahoma City, OK 73104-5046; and [7]Department of Biochemistry and Molecular Biology, University of Oklahoma Health Sciences Center, Oklahoma City, OK 73104, USA

(Received January 18, 2005/Revised May 9, 2005/Accepted May 9, 2005/Online Publication July 22, 2005)

Gene expression profiles of HCC and surrounding non-cancerous tissues in rats fed a CDAA diet for 70 weeks, as well as normal liver tissues, were explored using an oligonucleotide microarray for 3757 genes. A total of 146 genes were identified as differentially expressed; the affected functions including metabolism, apoptosis, cell cycling, RNA splicing, Wnt signaling, reactive oxygen species-induced stress, and fibro/cirrhogenesis. The genes were found to fit into four distinct expression patterns after classification by hierarchical and *k*-means clustering procedures. Notably, genes within the same functional category tended to be found within the same cluster, thus gene functions appeared to be related to their expression patterns. For example, genes encoding receptors (Fisher's exact test, $P < 0.01$) and cytokines (Fisher's exact test, $P < 0.05$) were both enriched in a cluster characterized by low expression in HCC compared to their surrounding tissues. While some of the receptors in this cluster had cell-proliferative potential, others are known to be growth-suppressive. It was noted, however, that four of the 10 receptor genes encode G-protein-coupled receptors, for which growth-suppressive potential has been reported. The seven growth factors in the same cluster included two fibroblast growth factors. The current findings suggest the possibility that genes differentially expressed in this multistep carcinogenic model may be classified into relatively few clusters according to their expression patterns, and that these clusters may be associated with gene functional categories. (*Cancer Sci* 2005; 96: 414–424)

Hepatocellular carcinomas are common in Asia and Africa, and the incidence is increasing in Europe and North America. The prognosis for HCC is extremely poor. In human HCC, both genetic and epigenetic alterations have been detected with regard to particular genes such as *p53*, cyclin D, $p16^{Ink4}$, $p21^{Waf1/Cip1}$, *Rb*, β-catenin, mannose-6-phosphate/insulin-like growth factor II receptor (*M6P/IGF2R*), E-cadherin, cyclo-oxygenase (*COX*)-2, and telomerase reverse transcriptase (*hTERT*).[1–3] In addition to studies on individual genes, microarray technology has allowed the exploration of comprehensive changes in expression during HCC development. To gain insight into the overall picture, suitable animal models are necessary so that samples reflecting various stages of carcinogenesis can be collected. It should be noted, however, that in animal models featuring the use of chemical carcinogens, unavoidable carcinogen-specific molecular alterations may mask generic and essential changes. In addition, the major risk factor in human HCC has been established as being continuous chronic liver injury, which occurs in hepatitis virus infections.[1–3] Thus we have chosen to use an animal model that employs the administration of a CDAA diet, which induces HCC on a background of continuous hepatic injury and cirrhosis. It has been confirmed that this model resembles human carcinogenesis caused by chronic viral hepatitis, hemochromatosis, and Wilson's disease in many respects.[1–4]

The CDAA diet is hepatocarcinogenic in male rats of Fischer 344 and Wistar strains.[4] As with other diets deficient in choline and low in methionine (CMD diets), HCC are induced in the absence of chemical carcinogens. In the CDAA model, HCC occur at a high rate through the induction and growth of preneoplastic hepatocellular lesions, which are followed by progression to hepatocellular adenomas and subsequent conversion to malignancy.[4] Chronic feeding of CMD diets in rats has also been accepted as an animal model for nonalcoholic fatty liver disease/nonalcoholic steatohepatitis (NAFLD/NASH), a condition in which a substantial number of patients develop HCC.[5] Here we have performed microarray analyses to obtain gene-expression profiles for HCC and surrounding non-cancerous tissues in CDAA treated rats, as well as normal liver samples, so as to gain insight into the mechanisms of multistep hepatic carcinogenesis.

Materials and Methods

Ethical considerations. The experimental protocols were approved by the Animal Experimentation Committee of the Sasaki Institute prior to their execution. The experiment was conducted under monitoring by the committee in accordance with the National Institute of Health's Guidelines for the Care and Use of Laboratory Animals, Japanese Government Animal Protection and Management Law Number 105, and Japanese Government Notification on Feeding and Safekeeping of Animals Number 6.

Animals, diets and animal treatment. A total of 10 male 5-week-old Fischer 344 rats were purchased from Charles River Japan (Atsugi, Kanagawa, Japan). They were divided into two groups of five animals, housed in plastic cages with white-flake

[8]To whom correspondence should be addressed. E-mail: fuematsu@sasaki.or.jp
Abbreviations: CDAA, choline-deficient, L-amino acid-defined; HCC, hepatocellular carcinoma; NAFLD, nonalcoholic fatty liver disease; NASH, nonalcoholic steatohepatitis; RT-PCR, reverse transcription polymerase chain reaction.

doi: 10.1111/j.1349-7006.2005.00069.x

bedding in an airconditioned room (25 ± 3°C temperature, 55 ± 8% relative humidity, 10–12 times/h ventilation and 12-h dark/light cycle). They were used after a 1-week acclimation on basal diet (CRF-1, Oriental Yeast Corporation, Itabashi, Tokyo, Japan) and allowed free access to food and tap water throughout the acclimation and experimental periods. Bodyweight, food consumption, and water intake were monitored weekly. The CDAA diet was obtained from Dyets (Bethlehem, PA, USA).

After acclimation, group 1 rats were administered the basal diet, while group 2 rats were placed on the CDAA diet for 70 weeks and then killed. The livers were then macroscopically examined. Portions of group 1 livers, and the macroscopic tumors and surrounding non-cancerous tissues of group 2 livers were fixed in 10% neutrally buffered-formalin for 24 h, embedded in paraffin, processed for the routine HE staining procedure, and histologically examined. Remaining portions of these three types of liver tissues were immediately frozen in liquid nitrogen and stored at −80°C. Group 1 liver tissues, group 2 liver tissues from non-cancerous areas, and group 2 liver tissues from tumors (after being histologically diagnosed as HCC) were employed as normal liver (CON), surrounding non-cancerous liver (NC), and HCC samples (CA). The microarray and RT-PCR experiments and the subsequent data analysis were performed using five CON samples from individual group 1 rats and five matched pairs of NC and CA samples from individual group 2 animals.

RNA isolation and probe labeling. Total RNA from liver tissues was isolated using an RNeasy Midi kit (QIAGEN, Hilden, Germany) and its integrity checked by electrophoresis on 1% agarose-formaldehyde gels. Five micrograms of total RNA from individual samples were then labeled with Cy3 (Amersham Biosciences, Uppsara, Sweden) using a BD Atlas PowerScript Fluorescent Labeling kit (BD Biosciences Clontech, Palo Alto, CA, USA) according to the manufacturer's protocols.

Hybridization, scanning and quantification. Cy3-labeled probes were hybridized to Atlas Rat 3.8 I microarrays (BD Biosciences Clontech) containing 3757 genes for 16 h at 50°C. After hybridization, microarrays were washed, dried and scanned using a GMS 418 confocal laser scanner (Genetic MicroSystems, Woburn, MA, USA). Fluorescence intensities of the Cy3 channels were quantified using ImaGene 4.0 software (BioDiscovery, El Segundo, CA, USA).

Microarray analysis and annotation of gene function. Data analysis was performed using GeneSpring software, version 5.1 (Silicon Genetics, Redwood City, CA, USA), including appropriate statistics. Dividing by the median calculated from all of the signal intensities for the Cy3 in a given sample, the fluorescence signal for each gene was normalized and the expression ratio was then calculated by dividing the normalized signal by the median for each gene to offset differences in expression levels between genes. Values were displayed as average of five animal samples for the three groups and were then logged (base 10) for further analyses. Standard deviations of the normalized values were calculated for the three groups, and genes in which standard deviation was more than two for any of the three groups were excluded. Genes differentially expressed among the three tissue types were detected by one-way ANOVA ($P = 0.02$).

The functions of the genes were assigned referring to a table attached to Atlas Rat 3.8 I microarrays (BD Biosciences Clontech), and classified into 21 categories: cell surface antigens, transcription factors, cell cycle-related factors, cell adhesion receptors/proteins, extracellular transport/carriers, stress response proteins, membrane channels/transporters, extracellular matrix proteins, trafficking/targeting proteins, metabolism-related factors, post-translational modification/protein folding-related factors, translation-related factors, apoptosis-related factors, RNA processing/turnover/transport-related factors, DNA binding and chromatin proteins, cell receptors, cell signaling/extracellular communicating factors, intracellular transducers/effectors/modulators, protein turnover-related factors, cytoskeleton/motility proteins, and others. Statistical significance for frequencies of genes of each functional category in each cluster was assessed as follows: values of the other categories in the relevant cluster, values of the other clusters in the relevant category, and values of the other clusters in the other categories were all combined, and the resultant combined values were compared with the relevant value by Fisher's exact test for the 2 × 2 table.

Semi-quantitative RT-PCR. Semi-quantitative RT-PCR was performed for seven genes, at least one gene from each cluster. They were endothelin receptor B (*EDNRB*), zinc finger protein 265 (*ZNF265*), neurofibromatosis type 1 (*NF1*), hepatic nuclear factor 1/transcription factor 1 (*HNF1/TCF1*), leukemia/lymphoma related factor (*LRF*), cyclin L (*CCNL*), and lamin A (*LMNA*). cDNA was synthesized from 3 μg of total RNA using a First-Strand cDNA Synthesis kit (Amersham Biosciences) and oligo(dT)$_{18}$ primer according to the manufacturer's instructions. RT-PCR was carried out using the GeneAmp PCR system 9700 (Applied Biosystems, Foster City, CA, USA) and cycling conditions were 2 min at 94°C, followed by 30 cycles (25 cycles for β-*actin*) of 94°C for 30 s, 55°C for 30 s, and 72°C for 30 s. Forward and reverse primer sequences were: *EDNRB*, 5′-TTGATGTGATTACGTCGGAC-3′ and 5′-GGACTGTTTTTCCTCAAACG-3′; *ZNF265*, 5′-AGAAGTACTACATCTGCTAG-3′ and 5′-TTCCCAGTTGTCAGCTTTGC-3′; *NF1*, 5′-GTACACCAAATACCATGAGC-3′ and 5′-ATGAAGAGGGTGTTGTTGGC-3′; *HNF1/TCF1*, 5′-TGCACTAGAAAGGCTGCTTC-3′ and 5′-GGTTTCTTGCAGTACCGAGG-3′; *LRF*, 5′-TGGGCCGCCTGAATGTAGCG-3′ and 5′-GTATGTCAGTGGTGGCCATG-3′; *CCNL*, 5′-TAATAGGCGAAGTCGATCTG-3′ and 5′-CATCGTCACACTGCATATGG-3′; *LMNA*, 5′-ATGAGAGCAGGTCTGAAGCC-3′ and 5′-AAGCATGGCAGATTTGCCTC-3′; β-*actin* (used as control), 5′-TTGAACACGGCATTGTAACC-3′ and 5′-ATCTCTTGCTCGAAGTCTAG-3′. PCR products were analyzed on 2% agarose gels with ethidium bromide and subsequently underwent densitometry. The obtained values were then normalized to those for β-*actin*.

Western blotting. Western blotting was conducted using the liver samples. Liver tissues were homogenized in 5 volumes of extraction buffer (10 mM Tris-HCl, pH 6.8, 1% SDS) using a polytron homogenizer at setting 7 for 90 s. The homogenates were heated on boiling water for 5 min and centrifuged at 13 000 × *g* for 30 min. The supernatants were used for western blotting. Protein concentrations of the lysates were determined using a BCA protein assay kit (Pierce, Rockford, IL, USA). Samples containing 5 μg of protein were separated on 7.5% SDS polyacrylamide gel electrophoresis and transferred to Hybond-P PVDF membranes (Amersham Biosciences, Buckinghamshire, UK). The blots were blocked with 5% dried milk in PBS for 1 h, incubated with 1:200 dilution of rabbit anti-EDNRB polyclonal antibody (Chemicon International, Temecula, CA, USA), washed in 0.1% Tween 20 in PBS, and incubated with 20 000-fold diluted antirabbit donkey IgG conjugated with peroxidase (Amersham Biosciences). Both primary and secondary antibodies were diluted with 0.1% Tween 20 in PBS, and incubation was at room temperature for 1 h. The immunoreactive bands were detected using ECL Plus Western Blotting Detection Reagents (Amersham Biosciences).

Results

General findings. All rats survived until their scheduled killing in relatively healthy conditions, but the mean bodyweight of group 2 animals was lighter than that of group 1 animals (Table 1). Group 1 livers showed no particular pathological changes either macroscopically or histologically. All of group 2 livers were macroscopically yellowish-white and appeared cirrhotic with 1 or 2 large tumoral nodules with a dark color. The mean relative liver weight was greater in group 2 compared

Table 1. Final body and relative liver weights

Group	Treatment	Animal	Final bodyweight (g)	Relative liver weight (g/100 g bodyweight)
1	Control	1	456	3.26
		2	448	3.04
		3	462	2.78
		4	460	2.88
		5	450	3.12
		Mean	455	3.02
		Standard deviation	6	0.19
2	CDAA	6	416	5.12
		7	422	4.88
		8	418	4.66
		9	408	5.38
		10	404	4.72
		Mean	414*	4.95*
		Standard deviation	7	0.3

*Significantly different from the group 1-value ($P = 0.0079$ by the two-tailed Mann–Whitney non-parametric test).

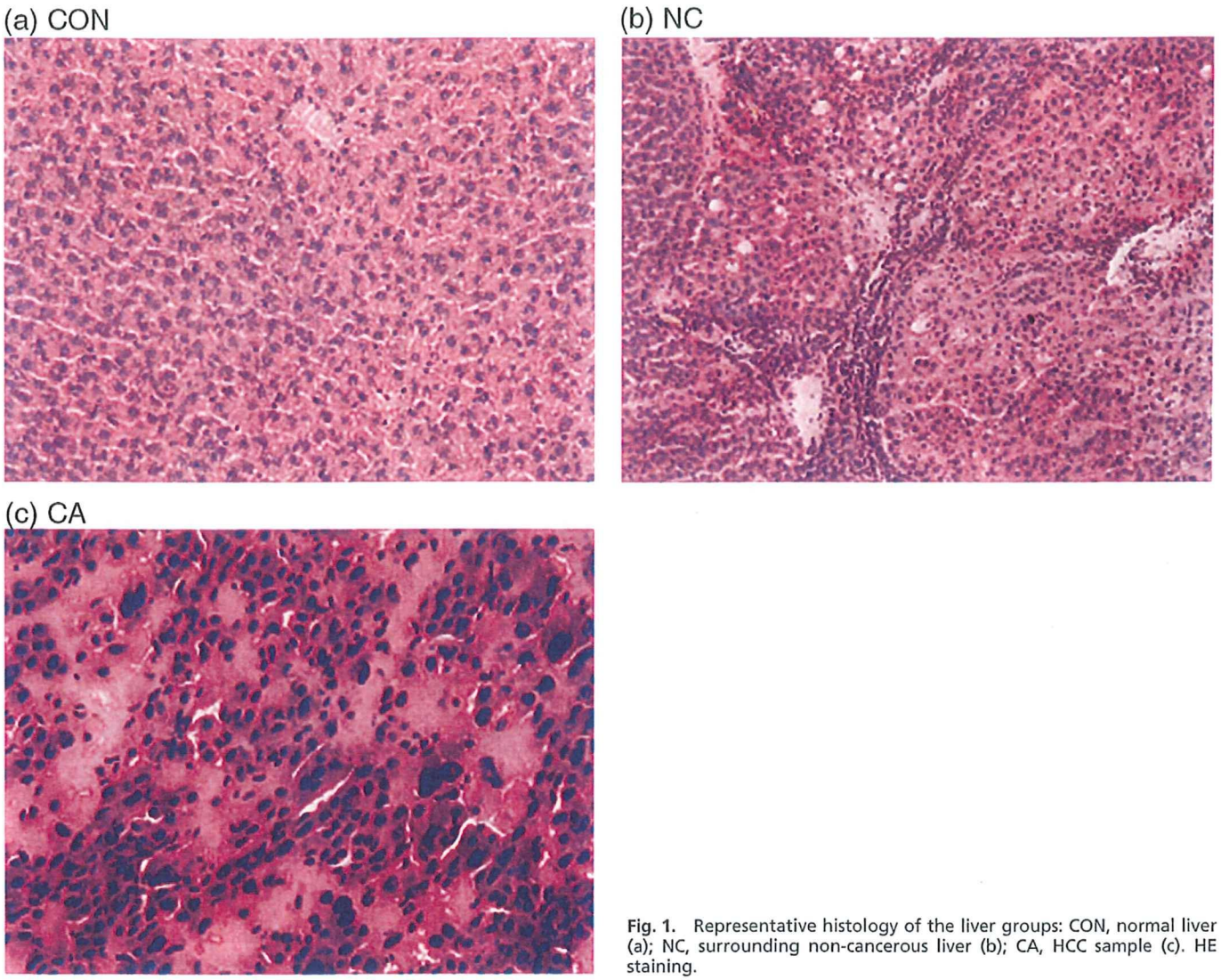

Fig. 1. Representative histology of the liver groups: CON, normal liver (a); NC, surrounding non-cancerous liver (b); CA, HCC sample (c). HE staining.

to group 1 animals (Table 1). Tumors were histologically diagnosed as relatively well-differentiated HCC, chiefly showing a trabecular pattern. The surrounding non-cancerous areas were cirrhotic, featuring intrahepatocellular fat accumulation, frequent hepatocellular apoptosis, and nuclear divisions of hepatocytes. These findings are in accordance with our previous results.[4] Representative histology of the three groups of liver samples is shown in Figure 1.

 doi: 10.1111/j.1349-7006.2005.00069.x

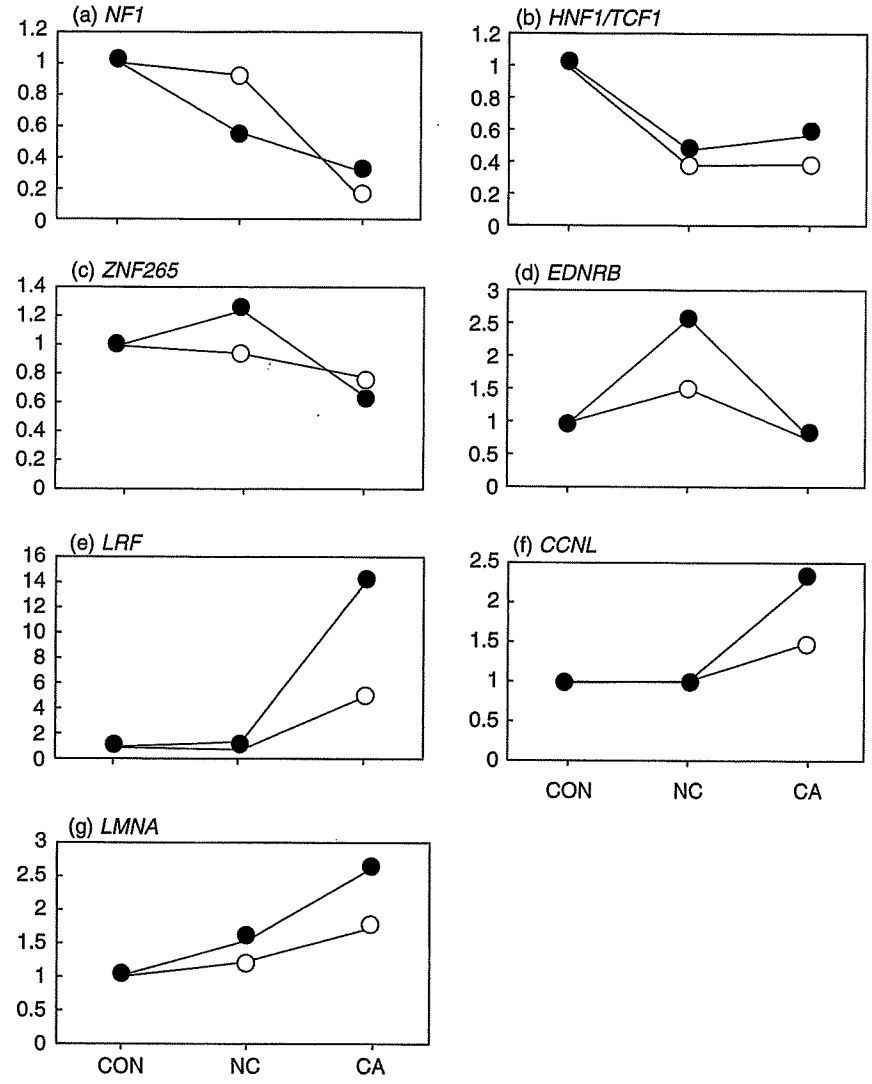

Fig. 2. Comparison of results obtained with microarray and semiquantitative RT-PCR for relative mRNA expression levels among normal liver (CON), surrounding non-cancerous liver (NC), and HCC samples (CA). The average expression levels of CON samples were set at 1. (○), data from RT-PCR; (●), data from microarray analysis. The indicated data for RT-PCR are from a single representative experiment, which was reproduced at least three times. (a), neurofibromatosis 1 (*NF1*); (b), hepatic nuclear factor 1/transcription factor 1 (*HNF1/TCF1*); (c), zinc finger protein 265 (*ZNF265*); (d), endothelin receptor B (*EDNRB*); (e), leukemia/lymphoma related factor (*LRF*); (f), cyclin L (*CCNL*); (g), lamin A (*LMNA*).

Changes in gene expression during carcinogenesis. We compared the gene expression profiles among CON, NC and CA using oligonucleotide microarrays containing 3757 genes. A total of 146 genes were detected as differentially expressed among the three tissue types. To verify the results of microarray analysis, expression of a total of seven genes (at least one gene from each cluster) was investigated by semiquantitative RT-PCR. These genes are involved in cell functions important in tumor progression, such as transcriptional regulation (*HNF1/TCF1* and *LRF*), RNA splicing (*ZNF265* and *CCNL*), signal transduction (*NF1* and *EDNRB*), and nuclear structure (*LMNA*) (Fig. 2). For comparison, the relative expression levels of CON were set to one. The expression patterns among the three sample groups were similar for these genes, although there are some discrepancies (Fig. 2). We considered that the results of microarray analysis were generally reproducible in RT-PCR, but the causes of the discrepancies are yet to be investigated.

Western blotting. In some cases, expression intensities at mRNA level and protein levels are not in parallel. So, we have investigated the expression levels of *EDNRB* by western blotting for comparison with data obtained by microarray and semiquantitative RT-PCR. At protein levels, the tendency of *EDNRB* expression was as follows: CON < NC > CA (Fig. 3a,b). So, in the case of *EDNRB*, changes in mRNA levels appear to be accompanied by changes in protein levels. High expression levels of *EDNRB* in rat[6] and human[7] liver cirrhosis compared to normal liver tissues have already been reported. The activated endothelin system can increase tonality of the hepatic microvasculature, which may contribute to the formation of liver cirrhosis.[6,7]

Detection of multiple patterns of expression with CON, NC and CA. Only the 146 genes that showed differential expressions were subjected to further analysis to prevent invariant genes from negatively affecting the clustering results. We first used a hierarchical clustering procedure and a dendrogram for classification of genes based on expression patterns (Fig. 4a). The genes were thereby divided along two major branches and then subdivided into two branches (Fig. 4a). Accordingly, we chose four for the total number of clusters in the subsequent *k*-means clustering analysis. The gene members contained in the four clusters obtained by *k*-means clustering were identical to those obtained by hierarchical clustering. We named them clusters 1–4, containing 18, 54, 45, and 29 members shown in Tables 2, 3, 4 and 5, respectively. Each of the four clusters had its own different pattern of expression profiles, with tendencies as follows: Cluster 1, CON > NC ≈ CA; cluster 2, CON < NC > CA [≈ CON]; cluster 3, CON ≥ NC < CA [> CON]; cluster 4, CON < NC < CA (Fig. 4b).

Gene function category of differentially expressed genes. In cluster 2, genes categorized as 'cell receptors' ($P < 0.01$) and 'cell signaling/extracellular communications' ($P < 0.05$) were significantly enriched. Genes in the categories of 'intracellular transducers' ($P < 0.05$) and 'cell receptors' ($P < 0.01$) were significantly low in clusters 1 and 3, respectively (Fig. 5).

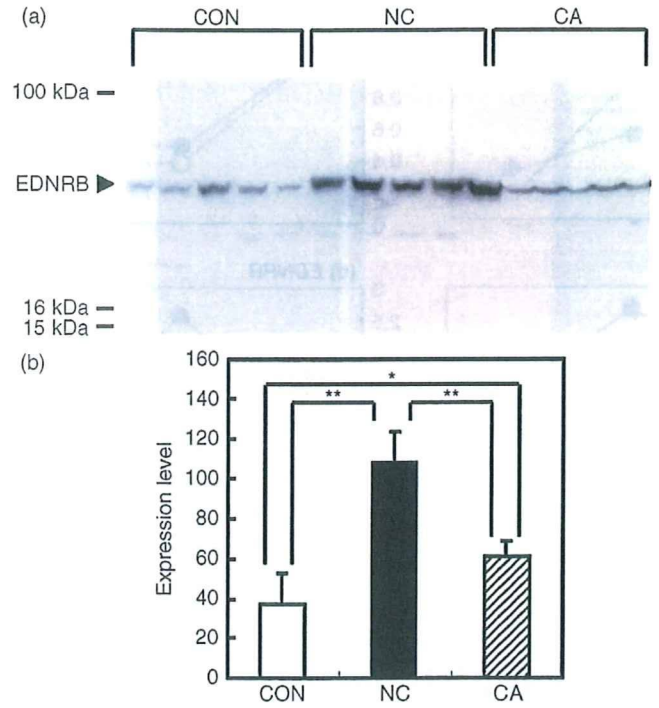

Fig. 3. (a) Expression of endothelin receptor B (*EDNRB*) detected in rat-liver samples by western blotting. (b) Protein levels of *EDNRB* compared between normal liver (CON), surrounding non-cancerous liver (NC), and HCC sample (CA). Data are expressed as mean ± SD in arbitrary units. There was a significant difference in expression levels among the three groups by ANOVA ($P < 0.01$). *$P < 0.05$ and **$P < 0.01$ by Student–Neuman–Keuls' test. The indicated data for western blotting are from a single representative experiment that was reproduced three times.

Discussion

Significance of the four clusters in hepatocarcinogenesis. The present results revealed that the gene expression profiles were differentially altered in HCC and their adjacent non-cancerous, cirrhotic liver tissues in rats. The differentially expressing genes could be divided into four clusters according to their expression patterns. Although we need to be cautious with the interpretation of these clusters, we speculate on the possible meanings of the expression patterns observed in the current study as follows. Genes belonging to cluster 1 were down-regulated in NC and also stayed low in CA, suggesting that the aberrant function of these genes may be involved in continuous liver injury, including fibro/cirrhogenesis, and early stage hepatocarcinogenesis. We have explored the expression of the cluster 1 gene *HNF1/TCF1* also by RT-PCR, and the roles of this gene in hepatocarcinogenesis are discussed further. Genes belonging to cluster 2 were upregulated in NC and then downregulated to the control level in CA, suggesting that the aberrant function of these genes is involved both in liver injury and hepatocarcinogenesis but with opposite influences. Alternatively, it is possible that these genes are necessary to be upregulated for liver injury but no longer have to be aberrantly expressed for carcinogenic processes. Genes belonging to cluster 3 were normally expressed in NC but then upregulated in CA, suggesting that the function of these genes may not be involved in liver injury but mainly in hepatocarcinogenesis. Genes belonging to cluster 4 were upregulated in NC and further upregulated in CA, suggesting that the function of these genes is positively involved both in liver injury and in hepatocarcinogenesis. However, to fully understand the roles of differentially expressed genes, exploration of the sequential expression of these genes at more time points may be needed.

Genes in the category of 'cell receptors' enriched in cluster 2. The present study showed that genes differentially expressed among CON, NC and CA fit into relatively few clusters, each showing distinct expression patterns. Further analyses revealed that certain functionally categorized genes are enriched in some clusters (Fig. 5). Notably, genes categorized as 'cell receptors' and 'cell signaling/extracellular communication proteins' were both enriched in cluster 2 (Table 3), characterized by high gene expression levels in NC compared with CON or CA (Fig. 4b). The precise significance of this expression pattern is not clear at present, but at least four of the 10 receptors in this cluster,

Table 2. Genes of cluster 1

Category	Gene name	GenBank accession number	Expression ratio		
			CON	NC	CA
Cell surface antigens	CD48 antigen	X13016	1.59	1.13	0.74
Transcription factors	D site albumin promoter binding protein	J03179	1.28	0.61	0.46
	Hepatic nuclear factor 1/*TCF1*	J03170	1.66	0.62	0.66
Cell cycle-related factors	Synaptonemal complex protein 3	X75785	1.84	0.99	0.56
Cell adhesion receptors/proteins	Milk fat globule membrane protein/ O-acetyltransferase	D84068	1.57	0.44	0.63
Extracellular matrix proteins	Collagen type X α1	AJ131848	1.41	0.91	0.99
Metabolism-related factors	α-1,3-Fucosyltransferase	U58860	1.82	0.99	0.71
	UDP-GalNAc:polypeptide N-acetylgalactosaminyltransferase T5	AF049344	1.15	0.82	0.81
	Glucose-6-phosphatase	D78592	1.77	0.50	0.46
	Branched chain aminotransferase 1	AF165887	1.29	0.76	0.90
Post-translational modification/ protein folding-related factors	FK506-binding protein 1	D86641	1.95	0.57	1.12
	Ubiquitin-conjugating enzyme E2D 3	AB006852	1.41	0.76	0.64
Translation-related factors	Ribosomal protein S15a	X77953	1.47	0.79	1.10
Cytoskeleton/motility proteins	Keratin complex 1, acidic, gene 18	U67992	1.09	0.55	0.94
Others	Ras homolog enriched in brain	U08227	1.05	1.00	0.65
	Peptidyl arginine deiminase, type 3	D88034	2.05	0.42	0.59
	Prostatic binding protein	X05034	1.69	1.01	0.48
	Scrapie responsive gene 1	AJ132434	1.17	0.63	0.83

CON, normal liver; NC, surrounding non-cancerous liver; CA, HCC sample.

 doi: 10.1111/j.1349-7006.2005.00069.x

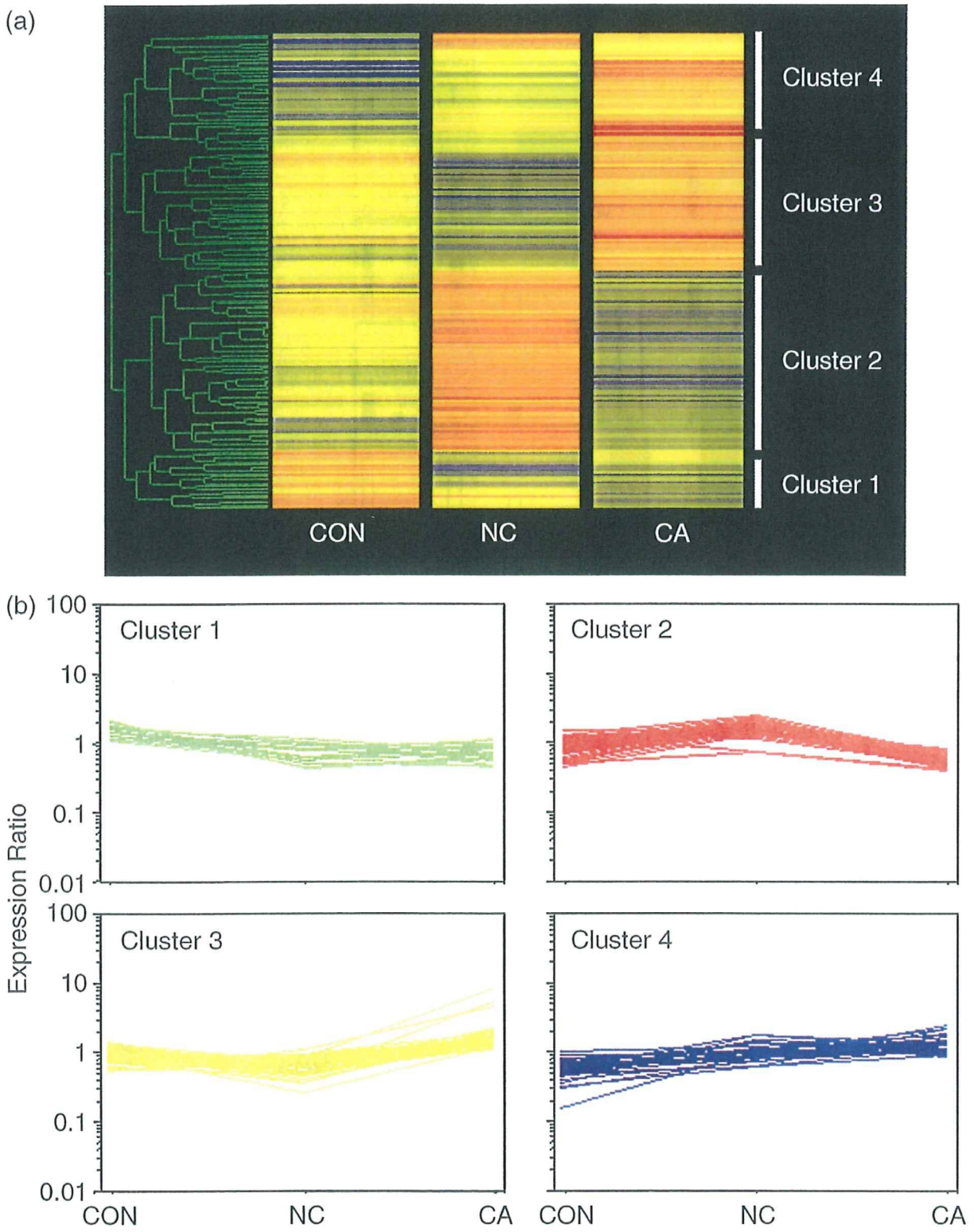

Fig. 4. Gene expression profiles among normal liver (CON), surrounding non-cancerous liver (NC), and HCC samples (CA). One hundred and forty-six genes were identified as demonstrating differential expressions among the three tissue types and subjected to further analysis. (a) Hierarchical clustering. A dendrogram is shown on the left side of the diagram. Tissue types are represented by columns and genes in rows. Red, yellow and blue represent the higher, equal and lower mRNA levels, respectively, relative to that of the median of each gene. The dendrogram indicates that data are divided along two main branches, each divides further into two branches. (b) Expression patterns of the genes included in the four clusters. The 146 genes were classified by hierarchical and *k*-means clustering procedures. Expression ratios of the genes are indicated.

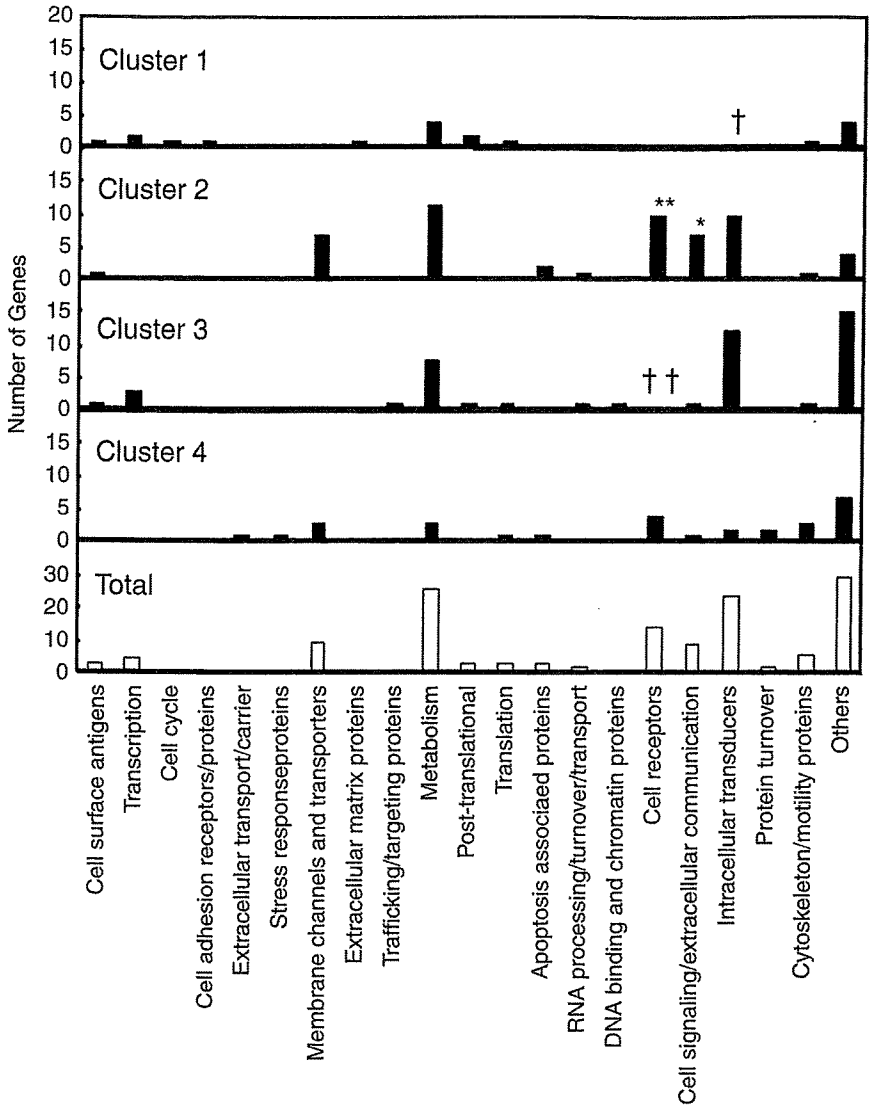

Fig. 5. Distribution of functionally categorized genes in each cluster. Numbers of genes within each functional category are shown. Frequency of each category in each cluster was evaluated by Fisher's exact test. Significantly elevated ($^{*}P < 0.05$, $^{**}P < 0.01$) and lowered ($^{\dagger}P < 0.05$, $^{\dagger\dagger}P < 0.01$) frequencies for genes in each cluster are indicated.

namely, opioid receptor κ1 (*OPRK1*), somatostatin receptor 1 (*SSTR1*), endothelin receptor A (*EDNRA*), and endothelin receptor B (*EDNRB*), are known for their inhibitory effects on cell growth.[8–11] This is in theoretical accordance with the downregulation of these genes observed between NC and CA (Fig. 4b, Table 3), as this would give cells a growth advantage. These four genes also belong to the same family, namely, G-protein-coupled receptors. In fact, the somatostatin and opioid systems are the main inhibitory systems in mammals, and relevant molecules including *OPRK1* and *SSTR1* have been under intense investigation in terms of their roles in tumorigenesis.[8–11] Moreover, downregulation of *EDNRB* has been studied in human prostate and nasopharyngeal cancer in relation to its abnormal methylation in CpG islands.[12,13] Another receptor gene, platelet derived growth factor receptor α (*PDGFRA*), however, is known for its growth-stimulating activity in certain types of cells. *TrkB*, a neurotrophic tyrosine kinase receptor, also found in this cluster, has recently been identified as a potent suppressor of anoikis and inducer of metastasis in epithelial cells.[14] *TrkB* and its ligand brain-derived neurotrophic factor are frequently coexpressed in human cancers, especially those with aggressive phenotypes,[15] suggesting the formation of an autocrine signaling pathway. So, while the expression patterns of the receptor genes in cluster 2 appear similar to each other, the cell signals related to each gene are diverse and should be individually explored.

Genes in the category of 'cell signaling/extracellular communications' enriched in cluster 2. Genes in the category of 'cell signaling/extracellular communications' were also enriched in cluster 2 (Fig. 5, Table 3). The seven genes included in this cluster encode polypeptide cytokines with various functions and related signal transduction systems after binding to their cognate receptors. It should be noted that fibroblast growth factor 5 (*FGF5*) and *FGF9*, both members of the FGF family, were found in this cluster. For FGF members stimulate growth and differentiation in a variety of cell types, and their roles in carcinogenesis have been investigated.[16] Hu *et al.* reported high expression levels of FGF1 in rat HCC induced by the Solt-Farber protocol.[17] In their results, FGF1 levels were elevated at early stages, decreased after one month, and remained low until the development of tumors. The reason why FGF5 and FGF9 were higher in NC rather than CA in the current study is not clear at present. However, there have been at least 23 FGF discovered thus far, and the roles of individual FGF in carcinogenesis have not been exactly elucidated.[16] Sequential expression analysis of these molecules during carcinogenesis may also help fully understand the roles of individual FGF in hepatocarcinogenesis.

 doi: 10.1111/j.1349-7006.2005.00069.x

Table 3. Genes of cluster 2

Category	Gene name	GenBank accession number	Expression ratio		
			CON	NC	CA
Cell surface antigens	CD36 antigen-like 2	M68965	0.73	2.10	0.67
Membrane channels/transporters	Inositol 1,4,5-triphosphate receptor 3	L06096	0.87	1.56	0.63
	X transporter protein 2	U12973	0.87	1.67	0.45
	ATPase, H^+K^+ transporting, non-gastric, α polypeptide	M90398	0.69	1.65	0.55
	Dopa decarboxylase	M27716	0.87	1.41	0.73
	Synaptotagmin 2	M64488	1.19	1.63	0.55
	Fatty acid binding protein 2	M35992	0.74	1.78	0.56
	Interleukin-2 receptor, β chain	M55050	1.15	1.44	0.55
Metabolism-related factors	Cytochrome P450 1B1	U09540	1.32	2.48	0.70
	Sucrose isomaltase	X15546	1.03	2.22	0.69
	Propionyl coenzyme A carboxylase, β polypeptide	M14634	1.30	1.56	0.62
	Mevalonate kinase	M29472	0.45	1.36	0.64
	Hexokinase 2	M68971	0.56	1.51	0.61
	Plasma glutathione peroxidase precursor	D00680	1.34	1.19	0.52
	Testis lipid binding protein	U07870	1.03	1.86	0.68
	Lactate dehydrogenase 3, C chain	U07177	1.01	1.41	0.71
	Solute carrier family 18, member 2	M97381	0.56	1.71	0.68
	Glycerol kinase	D16102	1.05	1.97	0.64
	Cytochrome P450 3A9	U60085	1.11	1.25	0.56
Apoptosis-related factors	Caspase 3	U49930	1.01	1.33	0.69
	α-Inhibin	M36453	1.18	1.50	0.83
RNA processing/turnover/ transport-related factors	Zinc finger protein 265	AF013967	1.18	1.47	0.78
Cell receptors	Opioid receptor, κ1	D16829	0.82	1.55	0.78
	Neural receptor protein-tyrosine kinase *TrkB*	M55291	0.51	1.42	0.67
	Somatostatin receptor subtype 1	X62314	1.01	2.15	0.58
	Platelet-derived growth factor receptor α	M63837	0.63	1.88	0.75
	Diphtheria toxin receptor	L05489	0.79	1.84	0.67
	Glutamate receptor, ionotropic, δ1	U08255	0.95	1.72	0.72
	Interleukin-1 receptor-like 1	U04317	0.72	1.70	0.45
	Endothelin receptor type A	X57764	0.60	1.53	0.50
	Interleukin-1 receptor, type I	M95578	0.80	1.47	0.56
	Endothelin receptor type B	M60786	0.93	1.56	0.54
Cell signaling/extracellular communicatimg factors	β-Nerve growth factor	M36589	0.54	1.72	0.81
	Cytokine-induced neutrophil chemoattractant-2	D21095	1.29	1.45	0.46
	Placental growth factor	L40030	0.96	1.90	0.42
	Neurotrophin-3	M34643	1.23	1.36	0.74
	Fibroblast growth factor-5	D64085	1.18	2.43	0.57
	c-fos induced growth factor	AF014827	0.97	1.82	0.66
	Fibroblast growth factor-9	D14839	0.76	1.92	0.65
Intracellular transducers/ effectors/modulators	Annexin 1/*p35*/lipocortin 1	M19967	1.04	1.37	0.61
	Insulin receptor substrate 1	X58375	1.03	1.67	0.77
	Neurofibromatosis type 1	D45201	1.32	0.75	0.40
	Phosphatidylinositol 4,5-bisphosphate 5-phosphatase, A	AB032551	0.84	1.48	0.47
	Endothelin converting enzyme-like 1	AB026293	0.85	1.79	0.79
	Src related tyrosine kinase	U09583	0.77	1.65	0.61
	S6 kinase	M58340	0.99	1.79	0.51
	Guanine nucleotide binding protein, γ7	L23219	1.11	1.44	0.78
	Polo-like kinase homolog	U10188	1.02	1.40	0.47
	Protein tyrosine phosphatase, non-receptor type 5	S49400	1.04	1.46	0.61
Cytoskeleton/motility proteins	Troponin 1, type 2	M73701	0.56	1.89	0.77
Others	P-glycoprotein/multidrug resistance 1	M81855	1.04	1.53	0.57
	Secretory zymogen granule membrane glycoprotein *GP2*	M58716	1.05	1.53	0.56
	Probasin	M27156	0.80	1.54	0.42
	Palmitoyl-protein thioesterase	L34262	0.51	2.30	0.62

CON, normal liver; NC, surrounding non-cancerous liver; CA, HCC sample.

Table 4. Genes of cluster 3

Category	Gene name	GenBank accession number	Expression ratio		
			CON	NC	CA
Cell surface antigens	MHC class II antigen RT1.B-1 β-chain	X56596	0.85	0.49	1.44
Transcription factors	Hepatic nuclear factor 4	D10554	1.09	0.60	1.56
	Mini chromosome maintenance deficient 6	U17565	1.04	0.71	1.46
	Leukemia/lymphoma related factor	D88450	0.62	0.83	8.57
Trafficking/targeting proteins	Clathrin, heavy polypeptide	J03583	1.25	0.60	1.58
Metabolism-related factors	Peroxiredoxin 6	AF110732	1.23	0.68	1.79
	Superoxide dismutase 3	Z24721	1.19	0.67	1.16
	Glutamate dehydrogenase	X14044	0.95	0.82	1.51
	Prostaglandin-endoperoxide synthase 1/cyclo-oxygenase 1	NM017043	0.73	0.63	1.12
	Dimethylglycine dehydrogenase precursor	X55995	1.01	0.49	1.72
	Hydroxyacid oxidase 3/glycolate oxidase 3	X67156	1.33	0.68	1.14
	Glycerol-3-phosphate dehydrogenase 2	X78593	1.27	0.45	1.55
	β-4N-acetylgalactosaminyltransferase	D17809	0.57	0.53	1.44
Post-translational modification/ protein folding-related factors	Peptidylglycine α-amidating monooxygenase	M25732	0.55	1.14	4.71
Translation	Eukaryotic translation initiation factor 2B, subunit 2	U31880	0.91	0.78	1.48
RNA processing/turnover/ transport-related factors	Cyclin L	AF030091	0.75	0.75	1.71
DNA binding and chromatin proteins	Histone H10	U49737	1.25	0.68	1.11
Cell signaling/extracellular communicating factors	Endothelin-2	U64949	1.03	0.55	1.17
Intracellular transducers/ effectors/modulators	Insulin receptor substrate 3	U93880	0.95	0.91	1.35
	PCTAIRE3	AB005541	0.81	0.37	2.07
	Calbindin 1	M31178	0.79	0.75	1.85
	Arrestin, β1	M91589	0.90	0.93	1.55
	Adenylyl cyclase 2	M80550	0.83	0.68	1.34
	Homeodomain-interacting protein kinase 3	AF036959	0.93	0.66	1.65
	Tuberous sclerosis 2	U24150	1.04	0.75	1.66
	AMP-activated protein kinase	Z29486	1.35	0.74	1.49
	Sialyltransferase 5	X76988	1.02	0.62	1.46
	Thyroid hormone receptor interactor 10	AB006914	0.58	0.67	1.81
	Peroxiredoxin 5	Y17295	1.02	0.87	1.47
	Sialyltransferase 8	U55938	1.10	0.68	2.16
Cytoskeleton/motility proteins	Kinesin heavy chain member 2	AF155824	0.91	0.76	1.21
Others	Cell growth regulatory with EF-hand domain	U66470	1.36	0.61	1.33
	Homeobox protein *R3*	M37567	1.01	0.55	2.28
	ADAMTS-1/METH-1	AF149118	0.94	0.67	1.29
	Outer mitochondrial membrane receptor *rTOM20*	U21871	1.01	0.94	1.92
	Coronin, actin-binding protein, 1B	AJ006064	1.41	0.53	1.40
	Unconventional myosin *Myr2* I heavy chain	X74800	0.98	0.86	1.41
	Replication factor C 2	AF208499	0.81	0.76	1.26
	Solute carrier family 29, member 1/*ENT1*	AF015304	0.94	0.55	1.47
	Aspartyl-tRNA synthetase/*DRS1*	U30812	1.16	0.50	1.16
	Quinoid dihydropteridine reductase	J03481	1.18	0.40	1.44
	Fibrinogen, γ-polypeptide	J00734	0.63	0.48	5.35
	Myosin light chain kinase 2	J03886	0.98	0.46	1.51
	Hyperpolarization-activated cyclin nucleotide-gated cation channel 1	AF247450	1.00	0.27	1.20
	ECL	X56190	0.79	0.50	1.57

CON, normal liver; NC, surrounding non-cancerous liver; CA, HCC sample.

Other deregulated genes associated with carcinogenesis. Metabolism-related factors found to be differentially expressed are mainly enzymes with a variety of functions and their genes did not show any significant enrichment in any of the four clusters (Fig. 5). Glucose-6-phosphatase is a negative phenotype marker of putatively preneoplastic foci of cellular alteration in the liver of rats,[18] and its activity is frequently lost also in human HCC.[19] CYP1B1 and CYP3A9 are both related to estrogen metabolism, and CYP enzymes are known as target genes of hepatic transcription factor 4 (HNF4). In human HCC, CYP enzymes are also generally down-regulated compared to surrounding tissues.[20] Aberrant expression of β-4N-acetylgalactosaminyl-transferase, observed here, is frequently detected in human HCC and other cancers.[21] Potassium voltage-gated channels play an important role in the proliferation and metastasis of HCC cells.[22]

 doi: 10.1111/j.1349-7006.2005.00069.x

Table 5. Genes of cluster 4

Category	Gene name	GenBank accession number	Expression ratio		
			CON	NC	CA
Extracellular transportors/carriers	Apolipoprotein A-V	AF202887	0.45	1.50	1.30
Stress response proteins	Solute carrier family 22, member 2/*OCT2*	D83044	0.52	0.64	0.95
Membrane channels/transporters	Solute carrier family 6, member 13/*GAT2*	M95762	0.73	1.38	1.14
	Chloride channel 1, skeletal muscle	X62894	0.60	1.77	1.39
	Potassium voltage-gated channel, subfamily H, member 2	Z96106	0.31	0.78	2.54
Metabolism-related factors	Protease 28 subunit, β/prosome/macropain	NM017257	0.33	0.66	2.28
	Protease, cysteine, 1/legumain	AF154349	0.51	1.04	1.32
	Malate dehydrogenase-like enzyme	AF093773	0.65	0.89	1.67
Translation-related factors	Ribosomal protein S2	U92698	0.78	1.10	1.13
Apoptosis-related factors	Lifeguard/neural membrane protein 35	AF044201	0.16	1.05	2.19
Cell receptors	Galanin receptor 3	AF073798	0.84	1.05	1.90
	Fc receptor, IgG, low affinity III	M32062	0.44	1.41	0.89
	Polymeric immunoglobulin receptor	X15741	0.40	0.74	1.33
	Neuromedin B receptor	U37058	0.36	1.76	1.17
Cell signaling/extracellular communicating factors	Glucose-dependent insulinotropic peptide	L08831	0.65	0.93	1.34
Intracellular transducers/ effectors/modulators	Phospholipase C, β3	M99567	0.67	0.86	1.32
	Thiol-specific antioxidant-like protein	AF053093	0.51	0.82	1.69
Protein turnover-related factors	Serine protease inhibitor	X16359	0.57	1.13	1.45
	Calpain, small subunit 1	U53859	0.55	0.94	1.65
Cytoskeleton/motility proteins	Actinin α1	AF115386	0.69	0.73	1.13
	Lamin A	X66870	0.56	0.87	1.47
	β-Spectrin 3	AB001347	0.64	0.85	1.15
Others	Thymosin, β10	M58404	0.55	1.42	1.07
	Solute carrier family 19, member 1/*RFC1*	AF099010	0.70	0.87	1.37
	Vitronectin	U44845	1.04	1.22	1.78
	Dendrin	X96589	0.91	0.96	1.05
	HLA-B-associated transcript 3	AB018791	0.75	0.97	1.08
	Rhodopsin/retinitis pigmentosa 4, autosomal dominant	Z46957	0.48	0.64	1.14
	Myosin heavy chain *Myr 8*	AF209114	0.59	0.95	0.98

CON, normal liver; NC, surrounding non-cancerous liver; CA, HCC sample.

In the CDAA diet model, repeated apoptotic death and proliferation of hepatocytes and fibro/cirrhogenesis have been shown to be important in the processes underlying hepatocarcinogenesis.[4,23] Genes with possible relation to fibro/cirrhogenesis included *PDGFRA*, diphtheria toxin receptor/heparin-binding epidermal growth factor receptor, *FGF5*, *FGF9*, interleukin *(IL)-1* receptor-like 1, *IL-1* receptor type *B*, *IL-2* receptor β-chain, *EDNRA*, *EDNRB*, endothelin converting enzyme-like 1, annexin 1/*p35*/lipocortin 1, insulin receptor substrate 1, *Src* related tyrosine kinase, and *S6* kinase.[24–28] Differentially expressed genes in the current study included both pro-apoptotic factors such as caspase 3 and α-inhibin,[29,30] and antiapoptotic factors such as calbindin 1, arrestin β1, homeodomain-interacting protein kinase 3, lifeguard, and lamin A.[31–35] Cyclin L[36] and ZNF265[37] are regulatory factors for the RNA splicing machinery so that their aberrant expressions may result in abnormal RNA splicing.

Reactive oxygen species-induced stress has been shown to be involved in human hepatocarcinogenesis,[1–3] NAFLD/NASH[5] and the rat CDAA diet model.[4,22] The present study detected the altered expression of several genes related to both anti- and pro-oxidative machinery, such as plasma glutathione peroxidase precursor, peroxiredoxins 5 and 6, superoxide dismutase 3, prostaglandin endoperoxide synthase 1/*COX-1*, phospholipase C β3, *and* thiol-specific antioxidant-like protein.

Our results have also shown aberrant expression of *HNF1/TCF1* and kinesin heavy chain member 2, two molecules involved in the Wnt signaling pathway, a major system involved in human hepatocarcinogenesis.[38] Biallelic inactivation of *HNF1/TCF1*, detected in human hepatic adenoma and HCC, is suspected to be important in early stages of liver tumor development.[39]

Regarding tumor-suppressor genes, the expression of both tuberous sclerosis 2 (*TSC2*) and its molecular target ras homolog enriched in brain (*Rheb*) was found to be altered in the current experiment. Neurofibromatosis type 1 (*NF1*) also exhibited variation between tissue types; and this may be the first report to suggest a potential involvement of *NF1* in HCC development. Other altered genes, fibrinogen γ-polypeptide, actinin α1 and vitronectin, have previously been reported to demonstrate corresponding changes in human hepatocarcinogenesis.[40,41]

Conclusion. Among the differentially expressed genes found in the present study, many have already been reported to have involvement in human and animal hepatocarcinogenesis. Statistical methods have proved useful for classifying these genes into relatively few clusters according to their expression patterns. Based on the functional classification of the differentially expressed genes, it was further indicated that these clusters may be associated with gene functional categories. For example, genes encoding the two major components of signal-transducing systems, cell receptors and cytokines, were significantly enriched in a particular cluster. Data have recently been accumulated regarding behaviors of individual tumor-related genes,[1–3] but mechanisms for global regulation of particular groups of genes are not fully understood. Several factors are supposed to affect overall behaviors of multiple genes. These include concordant methylation of CpG islands, which can result in suppression of multiple genes as described

in human cancers including HCC.[42] Although the causation of the association between expression patterns of genes and gene functional categories suggested in the current study is yet to be elucidated, these findings may give insight into underlying mechanisms for the evolution of HCC.

Acknowledgments

The authors thank Dr Yoshiyuki Hashimoto (Kyoritsu University of Pharmacy) for constant advice; Drs Tsuneyuki Oikawa (Department of Cell Genetics, Sasaki Institute), Tetsuya Muroya, and Masaru Sakamoto (Department of Gynecology, Kyoundo Hospital, Sasaki Foundation) for generous scientific supports; Drs Akihiko Maekawa (Sasaki Institute), Yashige Kotake (Free Radical Biology and Aging Research Program, Oklahoma Medical Research Foundation), and Yoichi Konishi (Nara Medical University) for helpful comments; Ms Hiromi Ichihara, Ms Hiromi Asako, and Ms Chinami Kajiwara (Department of Pathology, Sasaki Institute) for technical assistance. This work was supported by a Research Grant of the Princess Takamatsu Cancer Research Fund (01–23308), Grant of the Foundation for Promotion of Cancer Research, and Grant R01 CA82506 from the National Institute of Health of the USA.

References

1 Thorgeirsson SS, Grisham JW. Molecular pathogenesis of human hepatocellular carcinoma. *Nat Genet* 2002; **31**: 339–46.
2 Nita ME, Alves VAF, Carrilho FJ, Ono-Nita SK, Mello ES, Gama-Rodorigues JJ. Molecular aspects of hepatic carcinogenesis. *Rev Inst Med Trop Sao Paulo* 2002; **44**: 39–48.
3 Wang XW, Hussain SP, Huo TI *et al.* Molecular pathogenesis of human hepatocellular carcinoma. *Toxicology* 2002; **181–182**: 43–7.
4 Nakae D. Endogenous liver carcinogenesis in the rat. *Pathol Int* 1999; **49**: 1028–42.
5 Rinella ME, Green RM. The methionine-choline deficient dietary model of steatohepatitis does not exhibit insulin resistance. *J Hepatol* 2004; **40**: 47–51.
6 Yokomori H, Oda M, Ogi M *et al.* Enhanced expression of endothelin receptor subtypes in cirrhotic rat liver. *Liver* 2001; **21**: 114–22.
7 Yokomori H, Oda M, Yasogawa Y *et al.* Enhanced expression of endothelin B receptor at protein and gene levels in human cirrhotic liver. *Am J Pathol* 2001; **159**: 1353–62.
8 Hatzoglou A, Bakogeorgou E, Kampa M *et al.* Somatostatin and opioid receptors in mammary tissue. Role in cancer cell growth. *Adv Exp Med Biol* 2000; **480**: 55–63.
9 Lamberts SW, de Herder WW, Hofland LJ. Somatostatin analogs in the diagnosis and treatment of cancer. *Trends Endocrinol Metab* 2002; **13**: 451–7.
10 Ferjoux G, Bousquet C, Cordelier P *et al.* Signal transduction of somatostatin receptors negatively controlling cell proliferation. *J Physiol Paris* 2000; **94**: 205–10.
11 Panagiotou S, Bakogeorgou E, Papakonstanti E *et al.* Opioid agonists modify breast cancer cell proliferation by blocking cells to the G2/M phase of the cycle: involvement of cytoskeletal elements. *J Cell Biochem* 1999; **73**: 204–11.
12 Nelson JB, Lee WH, Nguyen SH, Jarrard DF, Brooks JD, Magnuson SR. Opgenorth TJ, Nelson WG, Bova GS. Methylation of the 5′-CpG island of the endothelin B receptor gene is common in human prostate cancer. *Cancer Res* 1997; **57**: 35–7.
13 Lo KW, Tsang YS, Kwong J, To KF, Teo PM, Huang DP. Promoter hypermethylation of the EDNRB gene in nasopharyngeal carcinoma. *Int J Cancer* 2002; **98**: 651–5.
14 Douma S, Van Laar T, Zevenhoven J, Meuwissen R, Van Garderen E, Peeper DS. Suppression of anoikis and induction of metastasis by the neurotrophic receptor TrkB. *Nature* 2004; **430**: 1034–40.
15 Aoyama M, Asai K, Shishikura T *et al.* Human neuroblastomas with unfavorable biologies express high levels of brain-derived neurotrophic factor mRNA and a variety of its variants. *Cancer Lett* 2001; **164**: 51–60.
16 McKeehan WL, Wang F, Kan M. The heparan sulfate-fibroblast growth factor family: diversity of structure and function. *Prog Nucleic Acid Res Mol Biol* 1998; **59**: 135–76.
17 Hu Z, Evarts RP, Fujio K *et al.* Expression of transforming growth factor alpha/epidermal growth factor receptor, hepatocyte growth factor/c-met and acidic fibroblast growth factor/fibroblast growth factor receptors during hepatocarcinogenesis. *Carcinogenesis* 1996; **17**: 931–8.
18 Williams GM. The significance of chemically-induced hepatocellular altered foci in rat liver and application to carcinogen detection. *Toxicol Pathol* 1989; **17**: 663–74.
19 Gerber MA, Thung SN. Enzyme patterns in human hepatocellular carcinoma. *Am J Pathol* 1980; **98**: 395–400.
20 Xu XR, Huang J, Xu XG *et al.* Insight into hepatocellular carcinogenesis at transcriptome level by comparing gene expression profiles of hepatocellular carcinoma with those of corresponding noncancerous liver. *Proc Natl Acad Sci USA* 2001; **98**: 15089–94.
21 Sugita Y, Fujiwara Y, Hoon DS *et al.* Overexpresion of beta 1,4N-acetylgalactosaminyl-transferase mRNA as a molecular marker for various types of cancers. *Oncology* 2002; **62**: 149–56.
22 Zhou Q, Kwan HY, Chan HC, Jiang JL, Tam SC, Yao X. Blockage of voltage-gated K^+ channels inhibits adhesion and proliferation of hepatocarcinoma cells. *Int J Mol Med* 2003; **11**: 261–6.
23 Nakae D, Uematsu F, Kishida H *et al.* Inhibition of development of hepatocellular carcinomas by phenyl *N-tert*-butyl nitrone in rats fed with a choline-deficient, 1-amino acid-defined diet. *Cancer Lett* 2004; **206**: 1–13.
24 Bonner JC. Regulation of PDGF and its receptors in fibrotic disease. *Cytokine Growth Factor Rev* 2004; **15**: 255–73.
25 de Coupade C, Gillet R, Bennoun M, Briand P, Russo-Marie F, Solito E. Annexin I expression and phophorylation are upregulated during liver regeneration and transformation in antithrombin III SV40 T large antigen transgenic mice. *Hepatology* 2000; **31**: 371–80.
26 Pinzani M, Marra F. Cytokine receptors and signaling in hepatic stellate cells. *Semin Liver Dis* 2001; **21**: 397–416.
27 Svegliati-Baloni G, Ridolfi F, Di Sario A *et al.* Insulin and insulin-like growth factor-1 stimulate proliferation and type I collagen accumulation by human hepatic stellate cells: Differential effects on signal transduction pathways. *Hepatology* 1999; **29**: 1743–51.
28 Vishwanath BS, Frey FJ, Escher G, Reichen J, Frey BM. Liver cirrhosis induces renal and liver phopholipase A_2 activity in rats. *J Clin Invest* 1996; **98**: 365–71.
29 Bredesen DE, Mehlen P, Rabizadeh S. Apoptosis and dependence receptors: a molecular basis for cellular addiction. *Physiol Rev* 2004; **84**: 411–30.
30 Chen YG, Lui HM, Lin SL, Lee JM, Ying SY. Regulation of cell proliferation, apoptosis, and carcinogenesis by activin. *Exp Biol Med* 2002; **227**: 75–87.
31 Castro CY, Stephenson M, Gondo MM, Medeiros LJ, Cagle PT. Prognostic implications of calbindin-D28k expression in lung cancer: Analysis of 452 cases. *Mod Pathol* 2000; **13**: 808–13.
32 Revankar CM, Vines CM, Cimino DF, Prossnitz ER. Arrestins block G protein-coupled receptor-mediated apoptosis. *J Biol Chem* 2004; **279**: 24578–84.
33 Kondo S, Lu Y, Debbas M *et al.* Characterization of cells and gene-targeted mice deficient for the p53-binding kinase homeodomain-interacting protein kinase I (HIP1). *Proc Natl Acad Sci USA* 2003; **100**: 5431–6.
34 Somia NV, Schmitt MJ, Vetter DE, Van Antwerp D, Heinemann SF, Verma IM. LFG: An anti-apoptotic gene that provides protection from Fas-mediated cell death. *Proc Natl Acad Sci USA* 1999; **96**: 12667–72.
35 Ho YS, Tsai PW, Yu CF, Liu HL, Chen RJ, Lin JK. Ketoconazole-induced apoptosis through P53-dependent pathway in human colorectal and hepatocellular carcinoma cell lines. *Toxicol Appl Phrmacol* 1998; **153**: 39–47.
36 Dickinson LA, Edgar AJ, Ehley J, Gottesfeld JM. Cyclin L is an RS domain protein involved in pre-mRNA splicing. *J Biol Chem* 2002; **277**: 25465–73.
37 Adams DJ, van der Weyden L, Mayeda A, Stamm S, Morris BJ, Rasko JE. ZNF265: a novel splicesomal protein able to induce alternative splicing. *J Cell Biol* 2001; **154**: 25–32.
38 Edamoto Y, Hara A, Biernat W *et al.* Alterations of RB1, p53 and Wnt pathways in hepatocellular carcinomas associated with hepatitis C, hepatitis B and alcoholic liver cirrhosis. *Int J Cancer* 2003; **106**: 334–41.
39 Bluteau O, Jeannot E, Bioulac-Sage P *et al.* Bi-allelic inactivation of *TCF1* in hepatic adenomas. *Nature Genet* 2002; **32**: 312–5.
40 Kondoh N, Wakatsuki T, Ryo A *et al.* Identification and characterization of genes associated with human hepatocellular carcinogenesis. *Cancer Res* 1999; **59**: 4990–6.
41 Nishiyama M, Ozturk M, Frohlich M, Mafune K, Steele G Jr, Wands JR. Expression of human alpha-actinin in human hepatocellular carcinoma. *Cancer Res* 1990; **50**: 6291–4.
42 Shen L, Ahuja N, Shen Y *et al.* DNA methylation and environmental exposures in human hepatocellular carcinoma. *J Natl Cancer Inst* 2002; **94**: 755–61.

 doi: 10.1111/j.1349-7006.2005.00069.x

Carcinogenesis vol.25 no.11 pp.2257–2264, 2004
doi:10.1093/carcin/bgh225

Dietary indole-3-carbinol promotes endometrial adenocarcinoma development in rats initiated with *N*-ethyl-*N'*-nitro-*N*-nitrosoguanidine, with induction of cytochrome P450s in the liver and consequent modulation of estrogen metabolism

Midori Yoshida[1,3], Sayumi Katashima[1], Jin Ando[1], Takuji Tanaka[2], Fumiyuki Uematsu[1], Dai Nakae[1] and Akihiko Maekawa[1]

[1]Department of Pathology, Sasaki Institute, Tokyo, Japan and [2]The First Department of Pathology, Kanazawa Medical University, Kanazawa, Japan

[3]To whom correspondence should be addressed
Email: midoriy@sasaki.or.jp

Indole-3-carbinol (I3C), found in cruciferous vegetables, has been shown to suppress or promote carcinogenesis depending on various animal models. Regarding its preventive effects, I3C acts as an anti-estrogen and can induce apoptosis, but precise mechanisms remain to be determined. Since I3C induces cytochrome P450 enzymes in the liver, it affects hydroxylation of estrogens and might therefore be expected to influence endometrial adenocarcinoma development. The present study was performed to clarify the effects of I3C using a rat two-stage endometrial carcinogenesis model, focusing on induction of cytochrome P450s and other estrogen-metabolic enzymes in the liver. First, to determine the estrogenic or anti-estrogenic activity, an uterotropic assay was conducted using ovariectomized Donryu rats (experiment 1). Second, to elucidate the effects on endometrial carcinogenicity, female Donryu rats initiated with a single dose of *N*-ethyl-*N'*-nitro-*N*-nitrosoguanidine into a uterine horn were fed 0 or 500 p.p.m. I3C in diets for 12 months (experiment 2). In experiment 3, similarly initiated animals received 0 or 2000 p.p.m. I3C in their diet, or 1 μg/kg 17β-estradiol (E2) or 5 μg/kg 4-hydroxyestradiol (4HE) subcutaneously twice a week for 12 months. In the uterotrophic assay, neither 500 nor 2000 p.p.m. of I3C showed any estrogenic or anti-estrogenic activity. In the two uterine carcinogenicity studies, I3C and 4HE increased incidences of uterine adenocarcinomas and/or multiplicities of uterine proliferative lesions, E2-treatment being associated with a tendency for promotion. In the liver, I3C treatment consistently elevated estradiol 2- and 4-hydroxylase activities, in particular the latter, but without effects on estradiol 16α-hydoxylase activity. mRNAs for CYP 1A1, 1A2 and 1B1 were increased by I3C treatment, with translation confirmed immunohistochemically. These results suggest that induction of the CYP 1 family in the liver and sequential modulation of estrogen metabolism to increase 4HE might play a crucial role in promoting the effects of dietary I3C on endometrial adenocarcinoma development.

Introduction

Indole derivatives are contained in cruciferous vegetables such as cabbage, broccoli, brussels, sprout and cauliflower (1). Indole-3-carbinol (I3C) is known to be an anti-estrogenic (2–4) or apoptosis-inducing compound (5), and has shown anticarcinogenic activity in a number of animal studies such as DMBA-induced rat mammary tumorigenesis (6) and spontaneous rat uterine adenocarcinoma development (7). I3C also has chemopreventive activity against benzo[*a*]pyrene-induced mouse forestomach carcinogenicity (8). It is neither cytotoxic, nor mutagenic *in vitro* (9,10), and thus I3C is a promising candidate for a chemopreventive agent against various tumors, especially estrogen-related examples. However, the compound has been documented to promote development of colon proliferative lesions in an animal model (11), and in a multi-organ rat model both inhibition and promotion were apparent, depending on the organ (12).

As for a hypothesized mechanism of chemopreventive effects of I3C, an anti-estrogenic and/or apoptosis-inducing effect have been widely accepted. In addition, the compound induces hepatic cytochrome P450s (CYPs) such as 1A1 and/or 1A2 (13–15), and increased activity of some phase I drug-metabolizing enzymes, including the CYP 1 family, can protect in some instances by increasing the rate of oxidation to less toxic metabolites (16–19). Recently I3C treatment was reported to also induce CYP 1B1 in the liver and/or other organs (20,21). In most animal species, it is well established that estradiol is metabolized by microsomal P450s in the liver and other organs/tissues, and that these enzymes therefore have the ability to modulate its effects (22–24).

In rats, CYP 1A2, 2B1/2B2 and 3A catalyze 2- or 4-hydroxylation of estradiol, mainly in the liver (24,25). In addition, evidence has recently been presented that CYP 1B1 is a major enzyme catalyzing 17β-estradiol (E2) to 4-hydroxyestradiol (4HE) (26). In the rat liver, E2 is metabolized by estradiol 2- and 4-hydroxylases into two types of catechol estrogens, 2-hydroxyestradiol (2HE) and 4HE, respectively. 2-Hydroxylation of estradiol is the dominant pathway for catechol estrogen formation (22,24), and 2HE can bind to the classical estrogen receptors, but with a markedly reduced binding affinity. This metabolite possesses much weaker hormonal potential than the parent hormone (27,28), and is not a carcinogenic agent (7,24,29). In contrast, 4HE, produced only in small amounts in the liver compared with 2HE, is hormonally active and can stimulate uterine growth by strong binding to estrogen receptors when injected into animals (24,26, 29–31). In addition, this catechol estrogen causes tumor development in the kidney in hamsters (23), and also has been implicated in uterine and mammary tumor development in human beings (32,33).

Much attention has been paid to modulation of estrogen metabolism by chemicals such as phenobarbital, dexamethasone, 3-methylcholanthrene and environmental pollutants via

Abbreviations: CYP, cytochrome; E2, 17β-estradiol; ENNG, *N*-ethyl-*N'*-nitro-*N*-nitrosoguanidine; 2HE, 2 hydroxyestradiol; 4HE, 4-hydroxyestradiol; I3C, indole-3-carbinol; PE, persistent estrus.